

AD 676276

# On Optimum Space Diversity Reception Of Correlated Multipath

By

Jim H. Derryberry and William D. Gregg

Department of Electrical Engineering

Technical Report No. 50

June 14, 1968

DDO  
OCT 22 1968  
RESOURCES  
R.

INFORMATION SYSTEMS RESEARCH LABORATORY

This document has been approved  
for public release and sale; its  
distribution is unlimited.

ELECTRONICS RESEARCH CENTER

THE UNIVERSITY OF TEXAS AT AUSTIN

AUSTIN, TEXAS 78712

CLEARINGHOUSE  
Information Springs 3/72/181

ON OPTIMUM SPACE DIVERSITY RECEPTION  
OF CORRELATED MULTIPATH\*

By

Jim H. Derryberry\*\*  
William D. Gregg\*\*\*  
Department of Electrical Engineering

Technical Report No. 50  
June 14, 1968

INFORMATION SYSTEMS RESEARCH LABORATORY

ELECTRONICS RESEARCH CENTER  
THE UNIVERSITY OF TEXAS AT AUSTIN

Austin, Texas 78712

- \* Research sponsored in part by the Joint Services Electronics Program under the Research Grant AF-AFOSR-766-67, Mod. 1 AFOSR-67-0766A and by the Bureau of Engineering Research, College of Engineering, The University of Texas at Austin
- \*\* Graduate Student, Candidate for M.S. Degree in Electrical Engineering
- \*\*\* Assistant Professor of Electrical Engineering, The University of Texas at Austin

This Document Contains  
Missing Page/s That Are  
Unavailable In The  
Original Document

OR are  
Blank pgs.  
that have  
Been Removed

**BEST  
AVAILABLE COPY**

## ABSTRACT

This research effort investigates system requirements, configurations, and associated performance characteristics of maximum-likelihood space-diversity receiving systems. From the maximum likelihood principle, and the multidimensional Karhunen-Loeve expansion, the continuous decision equations for space-time detection of noisy, random multipath signals are developed. Interpretation of these equations yields the optimum space-time receiving system configuration requirements.

The performance characteristics of the resultant systems are then analyzed to determine the effects of channel multipath structure (multipath delay and power division among the paths), space-time correlation properties of the incident processes, and the specific temporal correlation introduced by the array geometry. It is shown by a series of case studies, that for both the single element coupling as well as array multiple element coupling, that increasing the multipath delay factor results in decreased system performance capability for fixed power of the signal and noise processes. Similarly, the performance capacity is degraded as the available signal power tends to distribute more equally over the multiple transmission paths. These effects are attributed to the loss of effective signal energy concentration, resulting in a lower effective detectability signal-to-noise ratio. An investigation of these effects upon system performance, due to array geometry (receiving element spacing) shows that performance is enhanced by increasing the separation distance

...

of the elements for a given multipath situation. This phenomena is the result of a more compatible array beam pattern that comes about from increased spacing. In effect, with increased spacing, the main lobe of the pattern is narrowed, while the side lobes are optimally suppressed by the optimal cross-coupling of elements. Finally the analysis illustrates how optimum space-time receiving systems capability results from a joint consideration of the coupling and temporal processing, rather than dichotomization of the problem into a spatial (antenna) problem and a (temporal) data processing problem. As such, the analysis yields a more concise, broader, interpretation of system design requirements and associated performance characteristics.

## TABLE OF CONTENTS

	Page
ABSTRACT . . . . .	ii
LIST OF FIGURES . . . . .	vi
CHAPTER I - INTRODUCTION . . . . .	1
CHAPTER II - SYSTEM ENVIRONMENT AND PROCESS MODEL . . . . .	6
2-1 Multipath Structure . . . . .	7
2-2 Channel Process Model . . . . .	8
2-3 Hypothesis Structure . . . . .	15
CHAPTER III - OPTIMUM DECISION EQUATIONS AND SYSTEM CONFIGURATION . . . . .	17
3-1 Derivation and Decision Equations . . . . .	17
3-2 System Configuration . . . . .	23
3-3 Stationary Processes . . . . .	25
CHAPTER IV - SYSTEM PERFORMANCE . . . . .	35
4-1 True Distribution of the Test Statistic . . . . .	36
4-2 Calculation of True Mean and True Variance of L . . . . .	44
4-3 Gaussian Approximation for the Test Statistic Distribution . . . . .	46
4-4 Threshold Performance . . . . .	51
CHAPTER V - CASE STUDY . . . . .	55
5-1 Homogeneous Interference Assumption . . . . .	56
5-2 Case I - Single Element in Random Multipath Environment - Single Plane Wave Coherently Undetectable Case . . . . .	58

	Page
5-3 Case II - Two Element Array, No Multipath- Coherently Undetectable Case . . . . .	64
5-4 Case III - Two Element Array Correlated Multipath Structure, Coherently Undetectable Case . . . . .	76
5-5 Case IV - Multi-Element Array, Optimum Geometry, No Multipath . . . . .	90
5-6 Summary . . . . .	90
CHAPTER VI - CONCLUDING REMARKS AND FUTURE RESEARCH . . .	94
REFERENCES . . . . .	99

## LIST OF FIGURES

Figure	Page
1-1 General Optimum Space-Diversity Receiver Structure	3
2-1 Array Geometry	9
3-1 General Non-Stationary Receiver Structure	26
3-2 Two-Combiner Receiver Structure	26
3-3 Stationary Two-Receiving Element Structure	28
3-4 Stationary Two-Combiner Receiver Configuration	30
3-5 Estimator-Correlator Receiver Structure	33
3-6 Simplified Single Combiner Receiver Structure	33
5-1 Single Receiving Element Receiver Structure	59
5-2 Detectability Performance for Single Element with Multipath	62
5-3 ROC for Single Receiving Element System with Multipath	65
5-4 Two-Element Receiving System (Single Combiner)	68
5-5 ROC for Two-Element Receiver with Cross-Element Correlation	70
5-6 Two-Element Array Beam Pattern (Broadside Signal)	74
5-7 Two-Element Array Beam Pattern (Signal Incident at $30^\circ$ )	75
5-8 Effects upon Detectability of Multipath Structure	77
5-9 Effects upon ROC Resulting from Changing Multipath Delay	79

## List of Figures cont'd.

5-10	Effect upon Detectability of Increasing Per Cent of Signal Power in Second Multipath	80
5-11	Effect upon Detectability of Varying the Element Spacing	81
5-12	Effect upon ROC of Varying the Element Spacing	83
5-13	Comparison of Performance of 1 and 2 Element Receiver Configuration (Small $\Delta$ )	84
5-14	Comparison of Performance of 1 and 2 Element Receiver Configuration ( $\Delta=1$ )	85
5-15	Comparison of Performance of 1 and 2 Element Receiver Configuration ( $\Delta=4$ )	86
5-16	Comparison of Performance of 1 and 2 Element Receiver Configuration (Large $\Delta$ )	87
5-17	Receiver ROC for Multiple Elements, No Cross-Element Correlation, No Multipath	91

## CHAPTER I

### INTRODUCTION

In most modern communications/radar/sonar/seismology receiving systems, the concept of space diversity, or multi-element array reception, is of considerable importance.<sup>1, 2, 3</sup> In such a system, the receiver consists of an array of receiving elements, antennas, hydrophones, or geophones distributed in space. These elements couple the data processor to the electromagnetic or acoustic medium containing the desired information processes. It is through these spatially distributed elements that the spatio-temporal (space-time) wave function processes are transformed into temporal (time) voltage waveforms. Following the array elements is the receiver stage, which steers the beam pattern of the array in the direction of the incident information processes thus performing "beam steering" and "phasing" of the array. This stage, in addition to the array geometry, attempts to optimally exploit the spatial structure of the incident process (analogous to the temporal processing in the frequency filtering and combining stages of the data processor). Thus the array and its associated steering stages can be considered to be a spatial filter as well as a temporal data processor.

Following the spatial filter is the temporal data processor; it is here that the receiver performs operations (prediction, smoothing,

correlation, etc.) on the spatially filtered data to carry out the desired detection, classification, and estimation functions that yield the desired information (signal, no-signal; target, no-target; range, doppler, etc.).

Thus the total receiver structure shown in Fig. 1-1 consists of a spatial filter and a temporal filter. In order to attain "optimum" reception, one must treat the spatio-temporal processing jointly. Previous work has partitioned the over-all reception problem into a spatial solution (antenna array design, beam pattern synthesis)<sup>4, 5, 6</sup> and a temporal solution (classical statistical communication theory, detection theory, etc.)<sup>7, 8, 9, 10, 11, 12, 13</sup>. Recent studies<sup>14, 15, 16, 17, 18</sup> have shown the utility of working with the entire receiver system as a unit by considering the combined space-time receiving system operations to obtain optimum receiving systems with improved performance characteristics.<sup>19, 20, 21, 22, 23, 24</sup>

The temporal data processor can be either an analog system operating upon continuous waveforms or a discrete system in which the coupled processes are sampled (A/D conversion) at some stage and processed with a digital filter (digital computer).<sup>25</sup> The analysis that follows treats the waveform case and develops the expressions for the optimum continuous decision equations or test statistic computers. Interpretation of these equations yields the resulting optimum continuous, analog system configuration. This structure is highly dependent upon the second-order spatio-temporal properties of the incident processes, the spatial

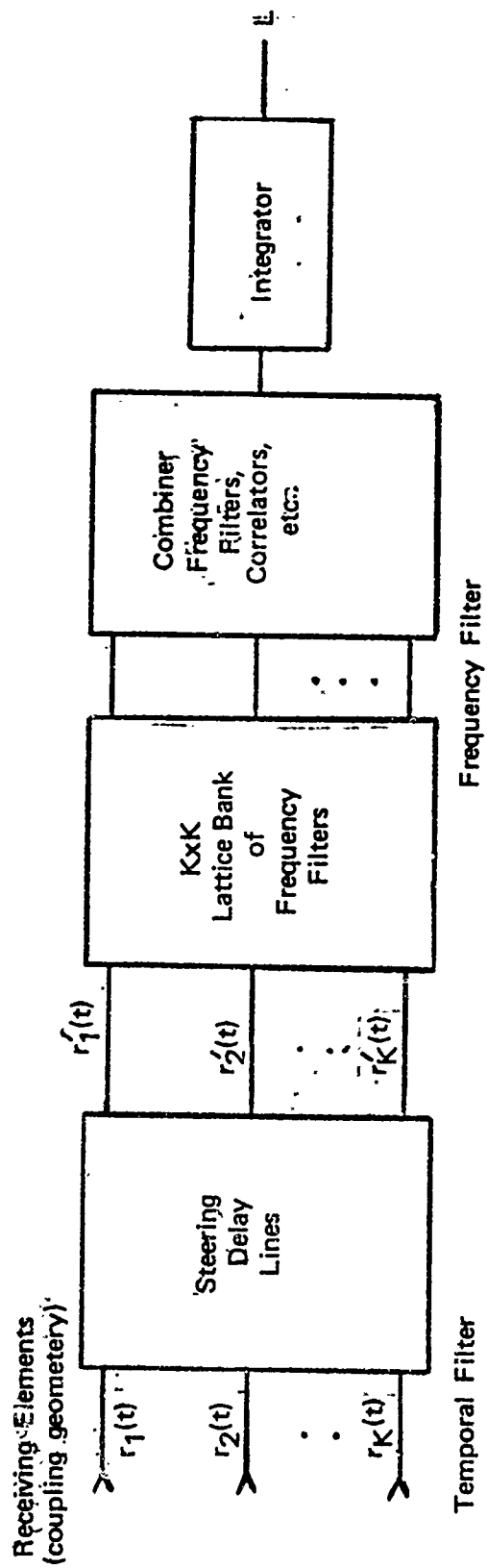


Fig. 1-1. General Optimal Space-Diversity Receiver Structure

filtering introduced by the array geometry, and the temporal filtering of the frequency filters, combining sections and beam forming stages.

In this research a model will first be developed for the information channel physics to which the receiver will be coupled. From this model the problem structure is formulated. Then, using the maximum likelihood principle,<sup>11, 12, 26, 27</sup> the coupled process expansion in orthogonal coordinates or sufficient statistics, and the Karhunen-Loeve series expansion for random processes, the space-time decision equations are developed. The performance characteristics of the resulting systems (detectability, and receiver operation characteristics) are then developed, analyzed, and interpreted. Finally, the performance for an array receiving system in a random multipath environment is presented to illustrate the effects of array geometry, the signal multipath structure, and the spatio-temporal properties of the incident random processes upon system performance. From such an analysis one obtains guidelines which enhance the design and implementation of more optimum detection estimation, classification and discrimination systems. The analysis and results are found in terms of process intensity, power, power spectra, array geometry, etc. Thus, this paper proposes to resolve, in terms of the parameters of physics (time, energy, and geometry) the problems:

1. For a given space-time structure of signal and interference processes, what is the optimum system configuration in terms of geometry and temporal structure?

2. For such systems, what are the expected optimum and actual (mis-matched) system performance characteristics ?

## CHAPTER II

### SYSTEM ENVIRONMENT AND PROCESS MODEL

The waveform processes incident upon the array of receiving elements consist of both noise and signal components. The noise components are due to a combination of all random interfering processes that exist within the receiving environment. Typical examples in the sonar case include sea noise, noises due to fish, noises due to other ships and submarines. The signal components are due to signals transmitted by the source, as in point-to-point communications, signals reflected by the target, as in active radar, sonar, seismology, or random signals propagated by the source as in passive radar/sonar or radio astronomy.

These signals can be either random, deterministic, or either with random or unknown parameters.<sup>11, 12, 13, 14</sup> This paper will treat the purely random signal case in which the incident signal components are assumed to be sample functions from a zero-mean (no specular component), gaussian process, produced by a channel or cross section containing multipath and a scattering mechanism. Such a random, multipath, information signal is commonly encountered in tropo-scatter communication links,<sup>28, 29</sup> telemetry links over randomly fading channels,<sup>30, 31</sup> and in sonar/radar detection-estimation media.<sup>7, 8, 9, 10, 14</sup> The multipath structure can arise from transmission through layered

media, as in the atmosphere in radar, or underground earth-rock layers as in seismology, in which parts of the signal are reflected and take different paths to the receiver array.<sup>29</sup> The random fading can occur in channels in which the transmission media is moving or varying in density, such as transmission of acoustic signals through the sea, etc.<sup>28</sup> Thus the received signal waveform can be classified as a random signal or a randomly faded, deterministic signal that has a scattering, multipath structure due to the channel media.<sup>21, 22, 24</sup> As such, this paper deals with the space-time (array) detection of a random, zero-mean, multipath signal in additive gaussian noise. The signal will be taken as purely random as is often encountered in passive radar, sonar, and radio astronomy.

## 2-1. Multipath Structure

The multipath structure will be assumed resolvable and characterized by delay  $\Delta$ .<sup>1, 7, 8, 30, 31</sup> This delay is due to the difference in transmission path length between source and receiver; it is assumed that the signals of each path arrive from the same direction with deviations from the angle of arrival small. The signal can be expressed as

$$z_{ch}(t) = \sum_{m=0}^{p-1} z_{ch_m}(t - m\Delta) \quad (2.1)$$

where  $p$  is the number of paths and  $\Delta$  is the characteristic delay.

## 2-2. Channel Process Model

The channel noise process is assumed taken as a zero-mean, gaussian process that additively masks the random signal waveform.

The total incident process is

$$r_{in}(t) = z_{ch}(t) + n_{ch}(t) \quad (2.2)$$

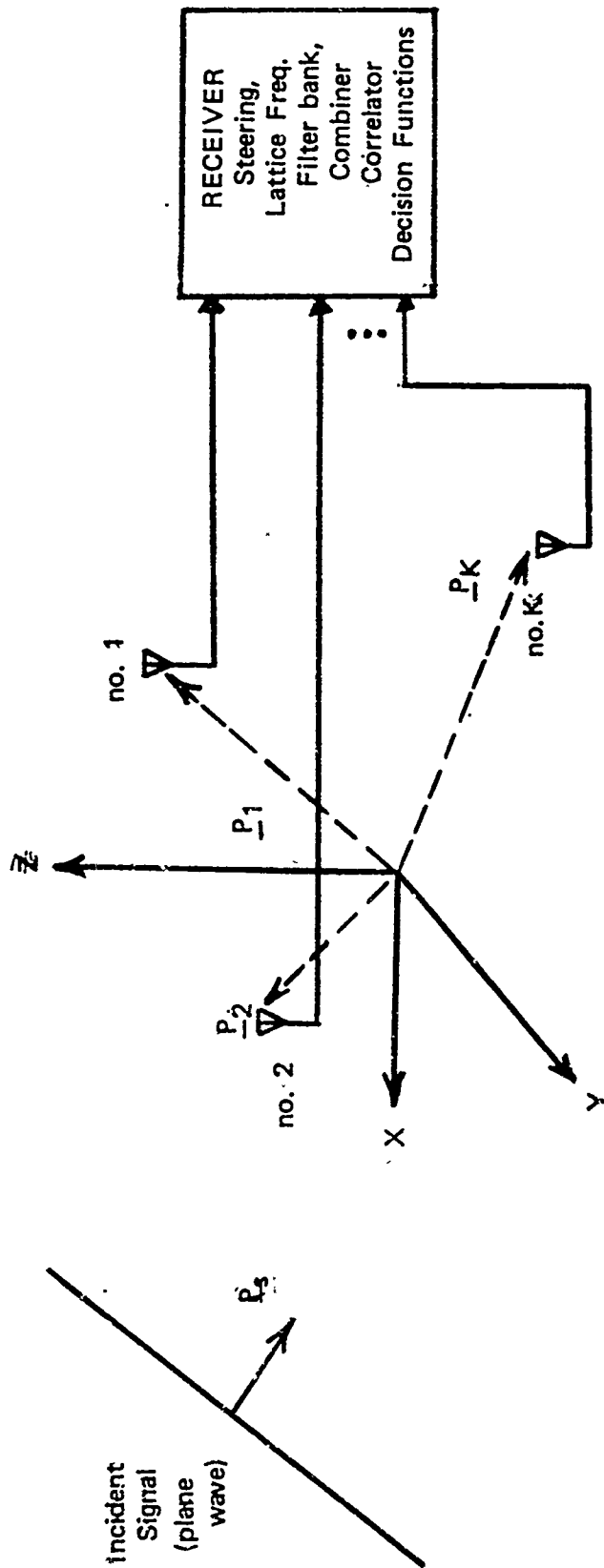
The random processes described above are incident upon an array of K elements distributed in space. The geometry is shown in Fig. 2-1. The location of each element relative to a known co-ordinate system is described by its respective position vector  $\underline{p}$ . The  $i$ th element is located in space at a point described by the vector  $\underline{p}_i$ .

$$\underline{p}_i^T = [p_{x_i} \ p_{y_i} \ p_{k_i}] \quad (2.3)$$

The incident wave interacts with the receiver elements to produce at the output terminals of each element a received process  $r(t)$ . The output of the  $i$ th element is  $r_i(t)$ . For a K element array, the set of output processes are written as the vector process

$$\underline{r}(t) = [r_1(t) \ r_2(t) \ \dots \ r_k(t)]^T \quad (2.4)$$

It is assumed that the process  $r_i(t)$  results from passage of the channel process through the receiver element with linear impulse response  $h_e(t, u)$ , allowing for imperfect receiving elements. The received process is thus



Receiving Elements (coupling geometry)  
Distributed in Space

Figure 2-1. Array Geometry

$$r_i(t) = \int_{t_0}^t h_e(t, u) r_{ch}(u) du \quad (2.5)$$

Each received waveform consists of a signal process plus a noise process. In addition there may be noise due to the receiver element or receiver "front end," which can be included as an additional post additive, coupling system noise process  $n_r(t)$ . Thus, the total received process at the output of the  $i$ th element is

$$x_i(t) = \int_{t_0}^t h_e(t, u) r_{ch}(u) du + n_{r_i}(t)$$

$$\triangleq z_i(t) + n_i(t) \quad (2.6)$$

where  $z_i(t)$  is the received signal component and the two noise processes can be added to produce the single noise interference  $n_i(t)$ . The set of received processes given in (2.4) is now

$$\underline{r}(t) = \underline{z}(t) + \underline{n}(t) \quad (2.7)$$

For the signal and noise independent, zero-mean, gaussian processes, the covariance function matrix of  $r(t)$  is defined as

$$\underline{K}_r(t, u) \triangleq E[\underline{r}(t) \underline{r}^T(u)] \quad (2.8)$$

with

$$\underline{K}_r(t, u) = \underline{K}_z(t, u) + \underline{K}_n(t, u) \quad (2.9)$$

where

$$\underline{K}_z(t, u) \triangleq E[\underline{z}(t) \underline{z}^T(u)] \quad (2.10)$$

and

$$\begin{aligned} \underline{K}_n(t, u) &\triangleq E[\underline{n}(t) \underline{n}^T(u)] \\ &= \frac{N_0}{2} \delta(t-u) \underline{I} + \underline{K}_c(t, u) \end{aligned} \quad (2.11)$$

The elements of the process covariance matrices can be termed self-correlation functions for elements on the diagonal of the covariance matrix and the off diagonal terms are a measure of the correlation in the processes between elements. Thus the correlation functions  $K_{r_{ij}}(t, u)$  can be denoted "self-link" correlation functions if  $i = j$  and "cross link" functions if  $i \neq j$ . The cross-link correlation functions are directly related to the spatial filtering produced by the array geometry in terms of the spatial correlation structure of  $\underline{r}(t)$ . This dependence results from the functions being dependent on the temporal variables and spatial variables (spatio-temporal correlation properties) of the incident process and upon the spatial variables of the array geometry.

The dependence upon array geometry can be seen by examining the received signal waveform vector  $\underline{r}(t)$ . Since the signal is assumed to be a plane wave with incidence angle unit vector  $\underline{p}_s$ , the wavefront is time delayed due to spatial distribution of the receiver elements.<sup>6, 8</sup> The received process in the  $i$ th element, located by the position vector  $\underline{p}_i$  is delayed by the amount  $\tau_i$ . The received signal vector is written

$$\underline{z}(t) = \begin{bmatrix} z_1(t) \\ z_2(t) \\ \vdots \\ z_k(t) \end{bmatrix} = \begin{bmatrix} z(t - \tau_1) \\ z(t - \tau_2) \\ \vdots \\ z(t - \tau_k) \end{bmatrix} \quad (2.12)$$

where  $\tau_i$  is given by the known wave front delay equation<sup>4, 5, 6</sup>

$$\tau_i = \frac{P_s \cdot P_i}{v} \quad (2.13)$$

with  $v$  the medium propagation velocity.

Using (2.12) and (2.10) gives

$$\underline{K}_z(t, u) = [K_{z_{ij}}(t - \tau_i, u - \tau_j)]$$

for all  $i, j \leq K$  (2.14)

The same analysis is valid for the noise correlation matrix. Thus the covariance matrices are functions of temporal and spatial variables and as such are proportional to the original spatio-temporal correlation functions. The general structure of such functions in terms of medium and aperture geometry have recently been investigated by Middleton.<sup>18, 32</sup>

The effects of the wave front delay of the signal components is counteracted by "steering" the array beam pattern. The array steering process is accomplished by passing each received process through an appropriate delay given by the negative of the wavefront delay. Thus, the  $i$ th process, after steering, becomes, the prime denoting the steered process

$$\begin{aligned}
 r_i^i(t) &= \int_{t_0}^{t_f} r_i(u) \delta(u-t-\tau_i) du = r_i(t+\tau_i) \\
 &= z_i(t-\tau_i+\tau_i) + n_i(t+\tau_i) \\
 &= z(t) + n_i(t+\tau_i) = z_i(t) + n_i^i(t).
 \end{aligned}
 \tag{2.15}$$

Similarly the jth steered process is

$$r_j^j(t) = z_j(t) + n_j(t+\tau_j) = z(t) + n_j^j(t) \tag{2.16}$$

The steering vector process is

$$\underline{r}^i(t) = \int_{t_0}^{t_f} \underline{H}_s(t, u) r(u) du$$

where the steering matrix  $\underline{H}_s(t, u)$  is a linear system with matrix impulse response

$$\underline{H}_s(t, u) \triangleq [\delta(u-t-\tau_i) \delta_{ij}]$$

The steered signal vector becomes, for homogeneous signal process

$$\underline{z}^i(t) = z(t) \underline{1} \tag{2.17}$$

and

$$\underline{n}^i(t) = [n_1(t+\tau_1) \ n_2(t+\tau_2) \ \dots \ n_k(t+\tau_k)]^T$$

The steering section of the receiver aligns the signal components of the received process and introduces a time shift in the received noise processes.

If both the signal and noise processes are stationary, the power spectrum of each can be found from the Fourier transform of the correlation function matrices.<sup>11, 12, 13</sup> Thus the  $ij$  element in the steered noise spectrum matrix is

$$\begin{aligned}
 S_{n'_{ij}}(\omega) &= \int_{-\infty}^{\infty} K_{n'_{ij}}(\tau) e^{-j\omega\tau} d\tau \\
 &= \int_{-\infty}^{\infty} K_{n_{ij}}(\tau + \tau_i - \tau_j) e^{-j\omega\tau} d\tau \\
 &= S_{n_{ij}}(\omega) e^{-j\omega(\tau_j - \tau_i)}
 \end{aligned} \tag{2.18}$$

where  $S_{n_{ij}}(\omega)$  is the  $ij$  element in the unsteered noise spectrum matrix. This term contains the variables  $\tau_i, \tau_j$  that are functions of the incident wave structure and the array geometry as given by equation (2.13). Thus the correlation function matrix, and its related power spectrum matrix, are proportional to the original spatio-temporal correlation functions and power spectral functions (bi-frequency and co-intensity).

The over-all effect of the steering stages is that of aligning the signal components, and simultaneously introducing new temporal correlation properties to the noise correlation matrix. The receiver structures will reflect these new properties and show the effects of altering the noise field space-time properties.

### 2-3. Hypothesis Structure

The hypothesis structure to be considered is the binary signal; no-signal case. Under hypothesis  $H_1$  the received process is the sum of signal and noise components

$$\underline{r}(t) = \underline{z}(t) + \underline{n}(t)$$

under  $H_0$  the received process is due to noise alone, thus

$$r(t) = n(t)$$

The correlation function matrix of  $r(t)$  under  $H_0$  is denoted

$$\underline{K}_0(t, u) = \underline{K}_n(t, u) \quad (2.19)$$

and under  $H_1$ , the correlation matrix is

$$\underline{K}_1(t, u) = \underline{K}_z(t, u) + \underline{K}_n(t, u) \quad (2.20)$$

The above model and hypothesis structure define the physical channel that is to be studied. The channel model is general enough to reflect the physical properties of a wide range of important information channels of technological interest.<sup>1, 18, 19</sup> The analysis of the detection problem receiver structures and system performance characteristics will reflect the model and hypothesis structure developed above. As such, the purpose of the research effort defined at the close of Chapter I will be realized as the optimum array (space-time) diversity detection

15

of noisy random, zero-mean, multipath, gaussian signals. The following chapter will derive the optimum decision equation for the channel model above.

CHAPTER III  
OPTIMUM DECISION EQUATIONS AND  
SYSTEM CONFIGURATION

The following chapter, using the previous channel model, establishes the optimum continuous likelihood ratio test (LRT)-decision equation for the array/diversity detection of random signals. After this relationship is established, the first and second moments (mean and variance) of the test statistic are found for stationary and non-stationary random processes. Interpretation of the LRT/decision equation yields the optimal array receiver structure. Several structures will be investigated.

3-1. Derivation of Decision Equations

Using the maximum likelihood principle,<sup>27, 11-14</sup> the expansion in independent coordinates of the likelihood ratio function defined as is initiated.

$$\hat{h}(\underline{r}(t)) = \frac{p(\underline{r}(t) | H_1)}{p(\underline{r}(t) | H_0)} \begin{matrix} > \eta & : & H_1 \\ < & : & H_0 \end{matrix} \quad (3.1)$$

For analysis purposes, let each of the above densities be the ratio of two densities, one of the density under  $H_1$  due non-white noise, and the other the density for  $r(t)$  white noise alone. Thus (3.1) becomes

10

$$\Lambda(\underline{r}(t)) = \frac{p(\underline{r}(t) | H_1)}{p(\underline{r}(t) | \text{white})} \cdot \frac{p(\underline{r}(t) | \text{white})}{p(\underline{r}(t) | H_0)} \quad (3.2)$$

The above densities are written in terms of independent co-ordinates by expanding the random process  $\underline{r}(t)$  in the vector Karhunen-Loeve expansion.<sup>33</sup> Thus (3.2) becomes

$$\Lambda(\underline{r}(t)) = \text{Lim}_{n \rightarrow \infty} \Lambda(\underline{r}_n) \quad (3.3)$$

where the independent co-ordinates under  $H_1$  are given by

$$r_i = z_i + n_i = \int_{T_i}^{T_f} \underline{r}^T(t) \underline{\psi}_i(t) dt$$

Under  $H_0$

$$r_i = n_i = \int_T^{T_f} \underline{r}^T(t) \underline{\psi}_i(t) dt \quad (3.4)$$

and

$$\lambda_i \underline{\varphi}_i(t) = \int_{T_i}^{T_f} \underline{K}_r(t, u) \underline{\psi}_i(u) du$$

where  $\lambda_i$  are the process eigenvalues and  $\underline{\psi}_i(t)$  are a set of orthonormal basis functions.<sup>33, 11-14</sup> The numerator term in independent co-ordinates becomes

$$\frac{p(\underline{r} | H_1)}{p(\underline{r} | H_w)} = \frac{\prod_{i=1}^{\infty} \frac{1}{\sqrt{2\pi} \sigma_{T_{1i}}} \exp\left(-\frac{1}{2} \left(\frac{r_i}{\sigma_{T_{1i}}}\right)^2\right)}{\prod_{i=1}^{\infty} \frac{1}{\sqrt{2\pi} \sigma_{T_{wi}}} \exp\left(-\frac{1}{2} \left(\frac{r_i}{\sigma_{T_{wi}}}\right)^2\right)} \quad (3.5)$$

The denominator is

$$\frac{p(\underline{r} | H_o)}{p(\underline{r} | H_w)} = \frac{\prod_{i=1}^{\infty} \frac{1}{\sqrt{2\pi} \sigma_{T_{O_i}}} \exp\left(-\frac{1}{2} \left(\frac{r_i}{\sigma_{T_{O_i}}}\right)^2\right)}{\prod_{i=1}^{\infty} \frac{1}{\sqrt{2\pi} \sigma_{T_{W_i}}} \exp\left(-\frac{1}{2} \left(\frac{r_i}{\sigma_{T_{W_i}}}\right)^2\right)} \quad (3.6)$$

where

$$\begin{aligned} \sigma_{T_{1_i}} &= \lambda_i^z + \frac{N_o}{2} + \lambda_i^c = \lambda_i^i + \frac{N_o}{2} \\ \sigma_{T_{O_i}} &= \frac{N_o}{2} + \lambda_i^c = \lambda_i^o + \frac{N_o}{2} \\ \sigma_{T_{W_i}} &= \frac{N_o}{2} \end{aligned} \quad (3.7)$$

and  $\lambda_i^z$  and  $\lambda_i^c$  are the eigenvalues of the signal and noise processes respectively. Truncating the infinite product at  $n$  and taking natural logarithms gives

$$L_n = \text{Ln} \Lambda(\underline{r}_n) = \left\{ \sum_{i=1}^n \text{Ln} \frac{\sigma_{T_{W_i}}}{\sigma_{T_{1_i}}} - \frac{1}{2} \sum_{i=1}^n \left( \frac{r_i^2}{\sigma_{T_{1_i}}^2} - \frac{r_i^2}{\sigma_{T_{W_i}}^2} \right) \right\} \quad (3.8)$$

$$- \left\{ \sum_{i=1}^n \text{Ln} \frac{\sigma_{T_{O_i}}}{\sigma_{T_{W_i}}} - \frac{1}{2} \sum_{i=1}^n \left( \frac{r_i^2}{\sigma_{T_{O_i}}^2} - \frac{r_i^2}{\sigma_{T_{W_i}}^2} \right) \right\} \geq \text{Ln} \eta$$

Using the vector Karhunen-Loève expansion given in (3.4), and the eigenvalues defined in (3.7), the first bracket term ( $L_{1_n}$ ) in (3.8) is

$$\begin{aligned}
L_{1n} = & \sum_{i=1}^n \text{Ln} \left( \frac{1}{1 + \frac{N_0}{2} \lambda_i^1} \right) - \frac{1}{2} \iint_{T_i}^{T_f} r^T(t) \sum_{i=1}^n \frac{\psi_i(t) \psi_i^T(u)}{\frac{N_0}{2} + \lambda_i^1} \underline{r}(u) \, dt \, du \\
& + \frac{1}{2} \iint_{T_i}^{T_f} r^T(t) \sum_{i=1}^n \frac{\psi_i(t) \psi_i^T(u)}{\frac{N_0}{2}} \underline{r}(u) \, dt \, du \quad (3.9)
\end{aligned}$$

The second term  $L_{2n}$  is found in a similar manner to be

$$\begin{aligned}
L_{2n} = & \sum_{i=1}^n \text{Ln} \left( \frac{\frac{N_0}{2} + \lambda_i^0}{\frac{N_0}{2}} \right) - \frac{1}{2} \iint_{T_i}^{T_f} r^T(t) \sum_{i=1}^n \frac{\psi_i(t) \psi_i^T(u)}{\frac{N_0}{2} + \lambda_i^0} \underline{r}(u) \, dt \, du \\
& + \frac{1}{2} \iint_{T_i}^{T_f} r^T(t) \sum_{i=1}^n \frac{\psi_i(t) \psi_i^T(u)}{\frac{N_0}{2}} \underline{r}(u) \, dt \, du \quad (3.10)
\end{aligned}$$

Using (3.9) and (3.10), taking the limit of (3.8) as  $n$ , the number of coordinates approaches infinity, combining terms, and putting constant terms on the right side of the equation gives

$$\begin{aligned}
L = \lim_{n \rightarrow \infty} L_n = & -\frac{1}{2} \iint_{T_i}^{T_f} r^T(t) \left[ M_{\underline{1}}(t, u) - \frac{2}{N_0} \delta(t-u) I \right] \underline{r}(u) \, dt \, du \\
& + \frac{1}{2} \iint_{T_i}^{T_f} r^T(t) \left[ M_{\underline{0}}(t, u) - \frac{2}{N_0} \delta(t-u) I \right] \underline{r}(u) \, dt \, du \geq \eta' : H_1 \\
& < \eta' : H_0 \quad (3.11)
\end{aligned}$$

where  $\eta' \triangleq L_n \eta + \sum_{i=1}^{\infty} (1 + \frac{2}{N_0} \lambda_i^1) - \sum_{i=1}^{\infty} (1 + \frac{2}{N_0} \lambda_i^0)$  is the new threshold

and  $M_{\underline{1}}(t, u)$  and  $M_{\underline{0}}(t, u)$  are solutions to the integral equations

$$\int_{T_i}^{T_f} K_{\underline{1}}(t, u) M_{\underline{1}}(u, z) du = \delta(t-z) \underline{I}$$

$$\int_{T_i}^{T_f} K_{\underline{0}}(t, u) M_{\underline{0}}(u, z) du = \delta(t-z) \underline{I} \quad (3.12)$$

and defined

$$M_{\underline{1}}(t, u) \triangleq \sum_{i=1}^{\infty} \frac{\psi_i(t) \psi_i^T(u)}{N_0 + \lambda_i^1}$$

$$M_{\underline{0}}(t, u) \triangleq \sum_{i=1}^{\infty} \frac{\psi_i(t) \psi_i^T(u)}{N_0 + \lambda_i^0} \quad (3.13)$$

Following the method of Price<sup>7, 8, 9</sup> for the single sensor case, by

defining

$$M_{\underline{1}}(t, u) \triangleq \frac{2}{N_0} \left[ \delta(t-u) \underline{I} - W_{\underline{1}}(t, u) \right]$$

$$M_{\underline{0}}(t, u) \triangleq \frac{2}{N_0} \left[ \delta(t-u) \underline{I} - W_{\underline{0}}(t, u) \right] \quad (3.14)$$

it can be shown that the matrix filters  $W_{\underline{1}}(t, u)$ ,  $W_{\underline{0}}(t, u)$  are solutions of the following matrix integral equations

$$\frac{N_0}{2} \underline{W}_1(t, z) + \int_{T_i}^{T_f} \underline{K}_{c_1}(t, u) \underline{W}_1(u, z) du = \underline{K}_{c_1}(t, z)$$

$$\frac{N_0}{2} \underline{W}_0(t, z) + \int_{T_i}^{T_f} \underline{K}_{c_0}(t, u) \underline{W}_0(u, z) du = \underline{K}_{c_0}(t, z)$$
(3.15)

where

$$\underline{K}_{c_1}(t, z) = \underline{K}_z(t, z) + \underline{K}_c(t, z)$$

and

$$\underline{K}_{c_0}(t, z) = \underline{K}_c(t, z)$$
(3.16)

These equations are Fredholm Integral Equations of the second kind, and can be solved by the methods given in 34 and 35. Following this procedure, the optimum decision equation in terms of the matrix filters  $\underline{W}_1(t, u)$  and  $\underline{W}_0(t, u)$  is

$$L = \frac{1}{N_0} \int_{T_i}^{T_f} \int_{T_i}^{T_f} \underline{r}^T(t) \underline{W}_1(t, u) \underline{r}(u) dt du - \frac{1}{N_0} \int_{T_i}^{T_f} \int_{T_i}^{T_f} \underline{r}^T(t) \underline{W}_0(t, u) \underline{r}(u) dt du \underset{<}{\overset{\geq}{}} \eta'$$
(3.17)

This equation can be rewritten in terms of a single matrix filter  $\underline{M}_\Delta(t, u)$  as

$$L = \int_{T_i}^{T_f} \int_{T_i}^{T_f} \underline{r}^T(t) \underline{M}_\Delta(t, u) \underline{r}(u) dt du \underset{<}{\overset{\geq}{}} N_0 \eta'$$
(3.18)

where the integral equation for  $\underline{M}_\Delta(t, u)$  is

$$\int_{T_i}^{T_f} \underline{K}_1(t, z) M_{\Delta}(z, w) \underline{K}_n(w, u) dw dz = K_s(t, u) \quad (3.19)$$

Equation (3.10) is the optimum "coupled space-time" decision equation for detection of random signals in noise. Interpretation of equation (3.10) yields the optimum system configuration, the following section will show several interpretations. The decision equation is written in terms of the correlation properties of the incident processes and the filtering (space-time) properties of the array; the system requirement will reflect this same dependence.

### 3.2. System Configuration

The previous section developed the optimum decision equation (3.18) based upon the maximum likelihood principle for binary hypotheses. In the development the matrix  $M_{\Delta}(t, u)$  was referred to as a filter. Interpretation of equation (3.18) yields the optimum system configurations, with one such system employing the  $M_{\Delta}(t, u)$  filter to be discussed first.

Equation (3.18) can be rewritten as

$$L = \int_{T_i}^{T_f} \underline{r}^T(t) \int_{T_i}^{T_f} M_{\Delta}(t, u) \underline{r}(u) du dt \quad (3.20)$$

In this form the received data vector  $\underline{r}(t)$  is passed through a lattice filter bank (convolution) and is then correlated with the unfiltered data producing the test statistic L. The matrix filter is a K-lattice bank

(for  $K$  receiving elements) of filters. The system configuration is shown in Figure 3-1. If the incident processes are non-stationary, the filters required are time varying and can be realized in the Kalman form;<sup>37</sup> stationary processes at the input would require linear time invariant filters.

Another system configuration for the optimum receiver can be found by dividing  $M_{\Delta}(t, u)$  into two filters defined by

$$M_{\Delta}(t, u) \triangleq \int_{T_i}^{T_f} H_{\underline{w}}(t, z) Q_{\underline{n}}(z, u) dz \quad (3.21)$$

where

$$\int_{T_i}^{T_f} K_{\underline{n}}(t, z) Q_{\underline{n}}(z, u) dz = \delta(t-u) \underline{I} \quad (3.22)$$

Substitution of (2.31) into the integral equation and using equation (3.22) for the inverse noise kernel matrix  $Q_{\underline{n}}(z, u)$  yields the integral equation for  $H_{\underline{w}}(t, z)$ .

$$K_{\underline{z}}(t, u) = \int_{T_i}^{T_f} [K_{\underline{z}}(t, x) + K_{\underline{n}}(t, x)] H_{\underline{w}}(x, u) du \quad (3.23)$$

This equation is the  $K \times K$  matrix Wiener-Hopf equation,<sup>34, 35, 14</sup> and the matrix filter  $H_{\underline{w}}(t, u)$  is the minimum-means-square-estimation filter for the  $K$ -vector processes  $\underline{z}(t)$

$$\hat{\underline{z}}(t)_{\text{mmse}} = \int_{T_i}^{T_f} H_{\underline{w}}^T(t, u) r(u) du \quad (3.24)$$

Equation (3.18) can thus be rewritten using (3.21) as

$$\begin{aligned}
 L &= \iiint_{T_i}^{T_f} \underline{r}^T(t) H_w(t, \underline{x}) Q_n(\underline{x}, u) \underline{r}(u) dx dt du \\
 &= \int_{T_i}^{T_f} \underline{z}^T(t) \underline{x}(t) dt
 \end{aligned} \tag{3.25}$$

Defining

$$\underline{x}(t) \triangleq \int_{T_i}^{T_f} Q_n(t, u) \underline{r}(u) du \tag{3.26}$$

The test statistic computer is such that the best estimate of the random signal is correlated with the "whitened" data  $\underline{r}(t)$ . The system configuration is shown in figure 3-2 and consists of two lattice banks of filters. In the upper branch the received data vector is passed through the whitening filter  $Q_n(t, u)$  and correlated with the "Weiner" or Kalman (minimum-means-square-error) estimate of the random signal waveform  $\hat{z}(t)$ . Thus the receiver structure is a K-lattice bank "estimator-correlator" receiver.<sup>7, 8, 9</sup>

### 3-3. Stationary Processes

For the stationary process case, the above systems can be manipulated to show further dependence of the system structure upon the space-time properties of the incident random processes, of the array structure, and of the steering.

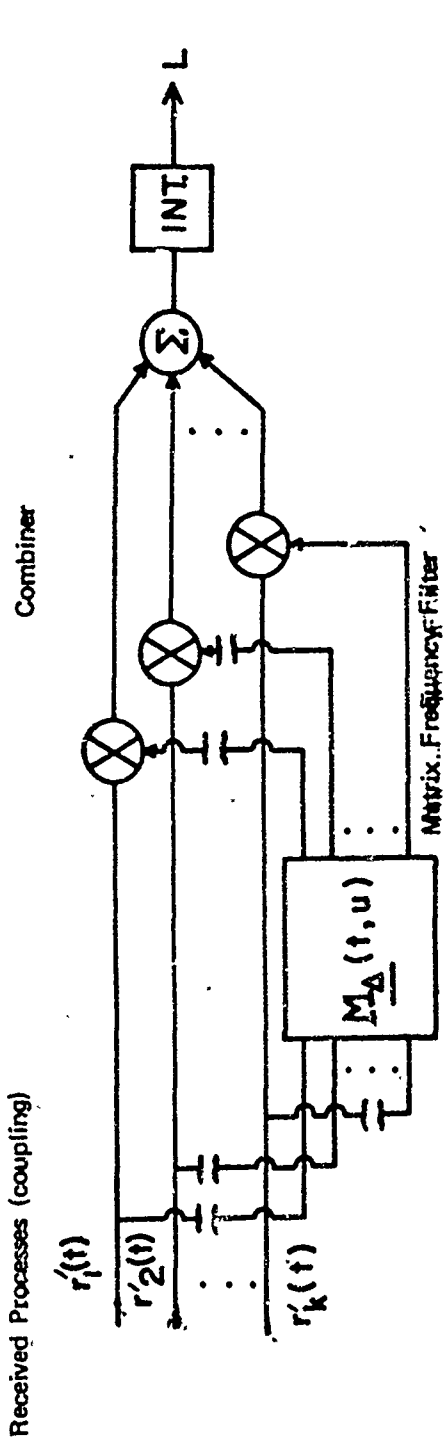


Fig. 3-1. General Receiver Structure, Interpretation 1.

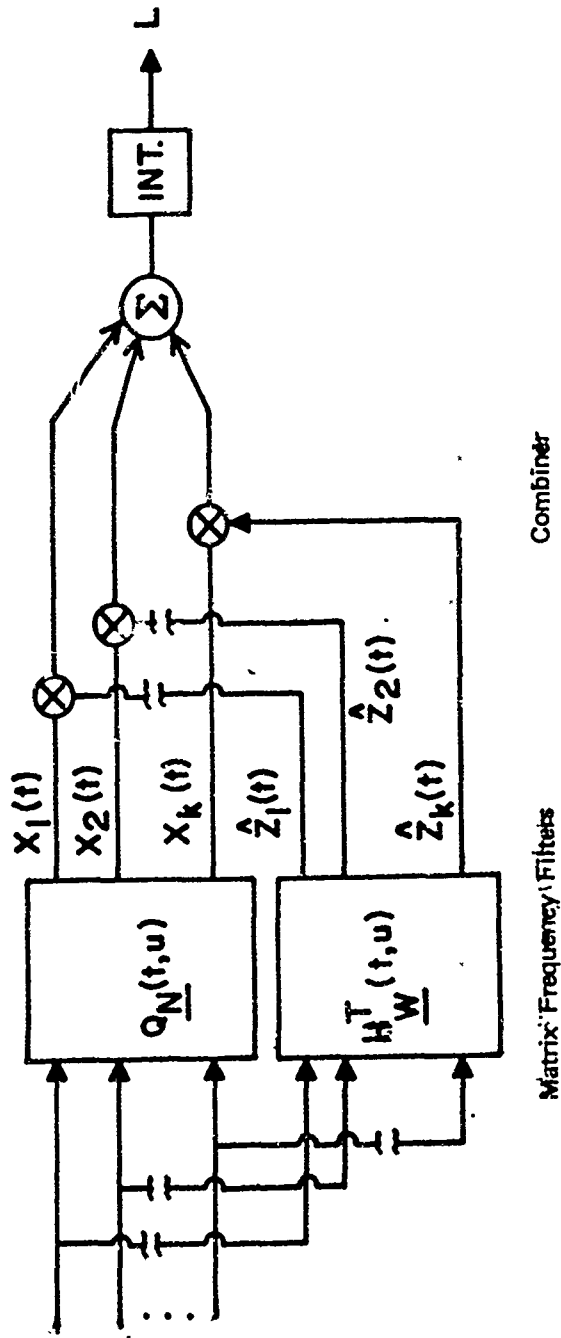


Fig. 3-2. Two-Combiner Receiver Structure, Interpretation 2.

The random processes are said to be stationary if the observation time  $T = T_f - T_i$  is greater than the reciprocal bandwidth of the random processes.<sup>26</sup> If such is the case, Fourier transformation of equation (3.19) yields the matrix frequency filter  $\underline{S}_Q(u)$  in terms of the process power spectra as

$$\underline{S}_Z(\omega) = \underline{S}_1(\omega) \underline{S}_Q(\omega) \underline{S}_n(\omega)$$

and

$$\underline{S}_Q(\omega) = \underline{S}_1^{-1}(\omega) \underline{S}_Z(\omega) \underline{S}_n^{-1}(\omega) \quad (3.27)$$

where  $\underline{S}_1(\omega)$ ,  $\underline{S}_Z(\omega)$ ,  $\underline{S}_n(\omega)$  were defined previously.

Employing the integrated transform<sup>14, 34, 35</sup> in equation (3.18), and using Parseval's theorem gives the test statistic  $L$  in frequency form.

$$L = \int_{-\infty}^{\infty} \underline{R}^{T*}(\omega) \underline{S}_Q(\omega) \underline{R}(\omega) \frac{d\omega}{2\pi} \quad (3.28)$$

Substitution of equation (3.27) into (3.28) gives

$$L = \int \underline{R}^{T*}(\omega) \underline{S}_1^{-1}(\omega) \underline{S}_Z(\omega) \underline{S}_n^{-1}(\omega) \underline{R}(\omega) \frac{d\omega}{2\pi} \quad (3.29)$$

The general stationary receiver structure is given by equation (3.29). K element case. A simplified structure for 2 elements is shown in figure 3-3.

Paralleling the development of equation (3.21) through (3.26) for the stationary case, gives

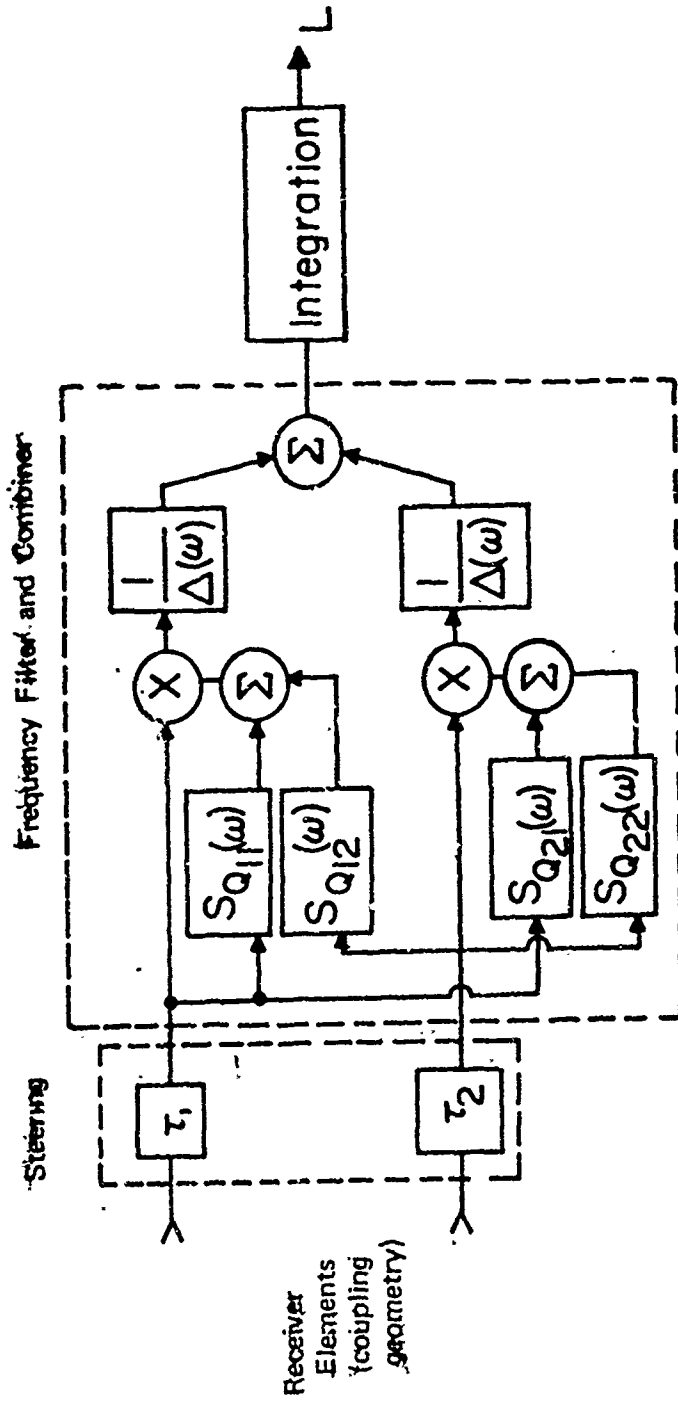


Figure 3-3. Stationary Two Receiver Element Structure

$$L = \int \underline{Z}^{T*}(\omega) \underline{X}(\omega) \frac{d\omega}{2\pi}$$

where

$$\underline{Z}(\omega) = \underline{S}_z(\omega) \underline{S}_1^{-1T}(\omega) \underline{R}(\omega) \quad (3.30)$$

$$\underline{X}(\omega) = \underline{S}_n^{-1}(\omega) \underline{R}(\omega) \quad (3.31)$$

This system shown in figure 3-4 is the frequency form of the structure shown in figure 3-2. It will be noted that this implementation again requires two matrix filters and combiners. Simplification results when the effects of array steering are exploited and utilized for the single signal case.<sup>14</sup>

It was shown previously that array steering caused the received waveform vector to undergo phase shifting due to array steering delays. Thus, after steering, the signal components are identical and

$$\underline{S}_{z'}(\omega) = \underline{S}_z(\omega) \underline{1} \underline{1}^T \quad (3.32)$$

and

$$\underline{S}_{n'}(\omega) = \left[ S_{n'_{ij}}(\omega) \right] \quad (3.33)$$

Thus, equation (3.30) becomes

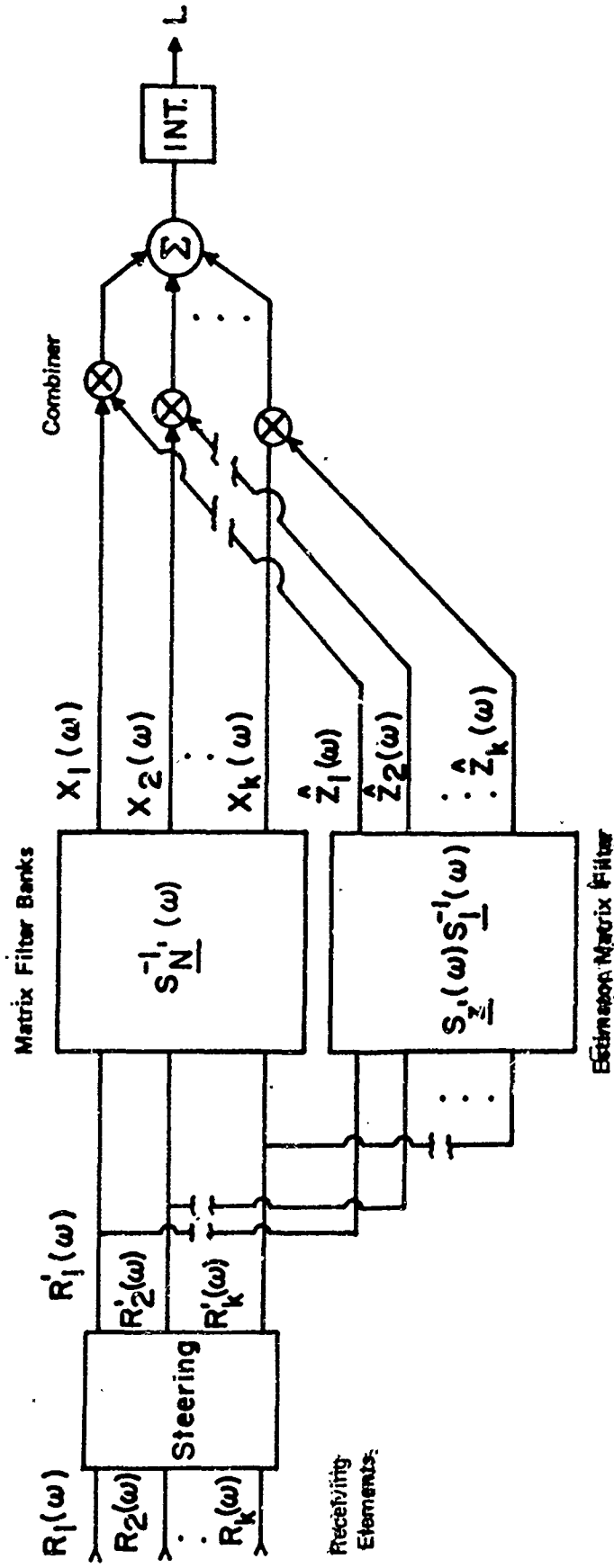


Fig. 3-4. Stationary Two-Combiner Receiver Structure, Interpretation 2.

$$\begin{aligned}
 \underline{Z}(\omega) &= S_z(\omega) \underline{1} \underline{1}^T S_{\underline{1}'}^{-1}(\omega) R'(\omega) \\
 &= S_z(\omega) \sum_i^K \sum_j^K S_{\underline{1}'}^{ij}(\omega) R'_j(\omega) \underline{1}
 \end{aligned} \tag{3.34}$$

where  $S_{\underline{1}'}^{ij}$  denotes the  $ij$ th element in the inverse of  $S_{\underline{1}'}(\omega)$ . Equation (3.29) becomes, using (3.33), (3.34)

$$\begin{aligned}
 L &= \int_{-\infty}^{\infty} S_z(\omega) \sum_i^K \sum_j^K S_{\underline{1}'}^{ij}(\omega) R'_j(\omega) \underline{1}^T S_{\underline{n}'}^{-1}(\omega) \underline{R}'(\omega) \frac{d\omega}{2\pi} \\
 &= \int_{-\infty}^{\infty} S_z(\omega) \sum_i^K \sum_j^K S_{\underline{1}'}^{ij}(\omega) R'_j(\omega) \sum_i^K \sum_j^K S_{\underline{n}'}^{ij}(\omega) R'_j(\omega) \frac{d\omega}{2\pi} \\
 &= \int_{-\infty}^{\infty} \hat{Z}(\omega) \sum_i^K X_i(\omega) \frac{d\omega}{2\pi}
 \end{aligned}$$

Thus the receiver reduces to that shown in figure 3-5. This structure can be simplified still further by showing that the scalar estimate  $\hat{Z}(\omega)$  can be produced by passing  $\sum_{i=1}^K X_i(\omega) = Y(\omega)$  through a linear filter  $T(\omega)$ . Mathematically, this is represented by

$$\hat{Z}(\omega) = T(\omega) Y(\omega)$$

Using the vector equations for  $\hat{Z}(\omega)$  and  $X(\omega)$

$$\hat{Z}(\omega) \underline{1} = T(\omega) X(\omega) = F(\omega) Y(\omega) \underline{1}$$

or

$$S_z(\omega) \underline{1} \underline{1}^T S_{\underline{1}'}^{-1}(\omega) \underline{R}'(\omega) = T(\omega) \underline{1} \underline{1}^T S_{\underline{n}'}^{-1}(\omega) R'(\omega)$$

$$\underline{S}_z(\omega) \underline{1}^T \underline{S}_{n'}^{-1}(\omega) = T(\omega) \underline{1}^T \underline{S}_{n'}^{-1}(\omega)$$

$$\underline{S}_z(\omega) \underline{1}^T \underline{I} = T(\omega) \underline{1}^T \underline{S}_{n'}^{-1}(\omega) \underline{S}_{1'}(\omega)$$

but

$$\underline{S}_{1'}(\omega) = \underline{S}_{z'}(\omega) + \underline{S}_{n'}(\omega)$$

Thus

$$\underline{S}_z(\omega) \underline{1}^T \underline{I} = T(\omega) \underline{1}^T \underline{I} + T(\omega) \underline{1}^T \underline{S}_{n'}^{-1}(\omega) \underline{S}_{z'}(\omega)$$

After simplification,

$$\underline{S}_z(\omega) = \left[ \underline{S}_z(\omega) \sum_{i=1}^K \sum_{j=1}^K S_{n'}^{ij}(\omega) + 1 \right] T(\omega)$$

Solving for the scalar frequency filter  $T(\omega)$  gives

$$T(\omega) = \frac{\underline{S}_z(\omega)}{1 + \underline{S}_z(\omega) \sum_{i=1}^K \sum_{j=1}^K S_{n'}^{ij}(\omega)} = \frac{\underline{S}_z(\omega)}{1 + N(\omega) \underline{S}_z(\omega)}$$

Thus the most easily implemented post-steering receiver structure passes the steered data through the  $K \times K$  matrix bank of frequency filters  $\underline{S}_{n'}^{-1}(\omega)$ , sums the outputs of the filter bank to form the scalar  $Y(\omega)$ , then passes  $Y(\omega)$  through the scalar linear system  $T(\omega)$ . The resulting estimate  $\hat{Z}(\omega)$  is correlated with  $Y(\omega)$  to form the test statistic  $L$ .<sup>14</sup> This system is shown in figure 3-6 and illustrates the dependence of the receiver structure on incident process spatio-temporal correlation properties, array geometry, and array steering.

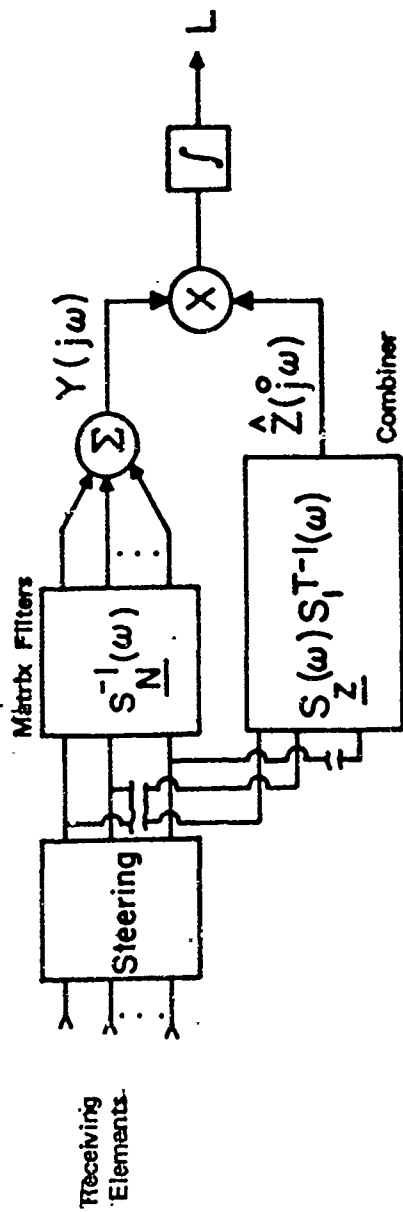


Fig. 3-5. Multilink Estimator-Correlator Receiver Structure

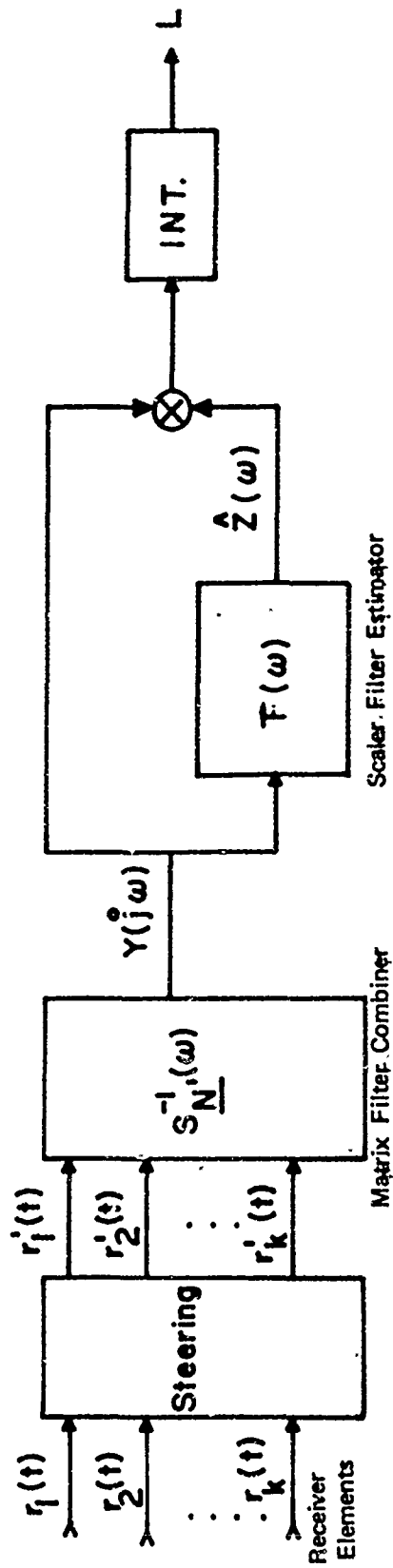


Figure 3-6. Simplified Single Combiner Receiver Structure

The optimum receiver structure can be found in the above manner for a given incident process structure.

The above sections have developed the optimum decision equations for the space-time detection of random signals in noise and have shown the optimum system configurations that result from an interpretation of these decision rules. The resulting systems were developed for the non-stationary and stationary steered case and were shown dependent upon the space time properties of the incident signal and noise fields, and array filtering characteristics. The next chapter investigates the performance of these systems.

## CHAPTER IV

### SYSTEM PERFORMANCE

Once the optimum receiver structures have been found, the performance of these systems must be evaluated. A performance measure for the preceding systems will be established and the nature of the test statistic  $L$  will be investigated.

To determine system performance characteristics, one needs the probability density of the test statistic  $L$ , under each hypothesis. From this density, false alarm probability,  $P_F$ , probability of detection,  $P_D$ , and error probabilities,  $P_E$ , can be defined and computed, thus specifying system performance.<sup>11-14, 26</sup>

The distribution of  $L$  under each hypothesis can be obtained in two ways. The first is a direct, exact probability density calculation; the second uses a gaussian approximation to the true distribution of  $L$ . In the approximation approach the density of  $L$  is taken to be gaussian, with true mean and true variance computed directly from the decision equation. The validity of this approximation has been considered and established by Price<sup>8, 36</sup> and Green<sup>36</sup>.

In both cases, the density of the test statistic under each hypothesis, and resulting performance probabilities will be shown to be dependent upon the spatio-temporal correlation properties of the

incident random processes, the array geometry and steering, and the receiver structure. Analysis of the performance measures will yield guidelines to enable one to improve the over-all system performance.

In this chapter, the true density will first be established, then the true mean and variance under each hypothesis will be computed. Using the true first and second moments the gaussian approximation will be made, invoking the Central Limit Theorem; and from the approximate densities the system performance criteria will be developed.

#### 4-1. True Distribution of the Test Statistic.

The optimum space-time decision function for the detection of random signals was given by equation (3.18) as

$$L = \int_{T_i}^{T_f} \underline{r}^T(t) M_{\underline{\Delta}}(t, u) \underline{r}(u) dt du \quad (4.1)$$

Expanding the continuous quadratic form, the decision equation becomes

$$\begin{aligned} L &= \int_{T_i}^{T_f} \sum_i^K \sum_j^K r_i(t) M_{\Delta_{ij}}(t, u) r_j(u) dt du \\ &= \sum_i^K \int_{T_i}^{T_f} r_i(t) M_{\Delta_{ii}}(t, u) r_i(u) dt du \\ &\quad + \sum_i^K \sum_{\substack{j \\ i \neq j}}^K r_i(t) M_{\Delta_{ij}}(t, u) r_j(u) dt du \end{aligned} \quad (4.2)$$

Defining

$$z_{ij}(t) = \int_{T_i}^{T_f} M_{\Delta_{ij}}(t, u) r_j(u) du \quad (4.3)$$

$$L = \sum_{i=1}^K \int_{T_i}^{T_f} r_i(t) z_j(t) dt + \sum_{\substack{i,j \\ i \neq j}}^K \int_{T_i}^{T_f} r_i(t) z_j(t) dt \quad (4.4)$$

Let the  $ij$  integral product of (4.4) be

$$L_{ij} \triangleq \int_{T_i}^{T_f} r_i(t) z_j(t) dt \quad (4.5)$$

Thus

$$\begin{aligned} L &= \sum_i^K L_{ii} + \sum_{\substack{i,j \\ i \neq j}}^K L_{ij} \\ &= L_{11} + L_{22} + \cdots + L_{kk} + L_{12} + \cdots + L_{k-1k} \end{aligned} \quad (4.6)$$

Examining a typical term in (4.6) shows that each  $L$  term is an infinite dimensional inner product. This is shown by taking the general term,  $L_{mp}$ , and expanding it in a series of orthonormal basis functions using the Karhunen Loéve expansion.

$$L_{mp} = \int_{T_i}^{T_f} r_m(t) z_p(t) dt \quad (4.7)$$

where  $1 \leq m, p \leq k$  and the processes can be written

$$r_m(t) = \sum_{i=1}^{\infty} r_{m_i} \psi_{m_i}(t)$$

$$z_p(t) = \sum_{i=1}^{\infty} z_{p_i} \psi_{p_i}(t)$$

where

$$z_{p_i} = \int_{T_i}^{T_f} z_p(t) \psi_{p_i}(t) dt \quad (4.8)$$

$$r_{m_i} = \int_{T_i}^{T_f} r_m(t) \psi_{m_i}(t) dt$$

Dropping the m, p subscripts gives for (4.7)

$$L = \int_{T_i}^{T_f} \sum_{i=1}^{\infty} \sum_{j=1}^{\infty} r_i z_j \psi_i(t) \psi_j(t) dt \quad (4.9)$$

Interchange of summation and integration and using the definition of orthonormal basis functions<sup>11-14</sup> yields

$$L = \sum_{i=1}^{\infty} \sum_{j=1}^{\infty} r_i z_j \delta_{ij} = \lim_{n \rightarrow \infty} \sum_{i=1}^n r_i z_i = \lim_{n \rightarrow \infty} L_n \quad (4.10)$$

where

$$L_n = \sum_{i=1}^n r_i z_i = \underline{r}^T \underline{z} \quad (4.11)$$

Thus using the n-truncation of (4.11), (4.6) can be written as a sum of inner products

$$L = \lim_{n \rightarrow \infty} \left( \sum_{i=1}^n L_{n_{ii}} + \sum_{i=1}^n \sum_{\substack{j=1 \\ i \neq j}}^n L_{n_{ij}} \right) \quad (4.12)$$

In the limit the products are infinite dimensional.

In order to find the density of  $L$ , one must find the density of the sum of  $K^2$  inner products. The mathematic is quite formidable, as the products  $L_{n_{ij}}$  are non-gaussian and not independent.<sup>40, 41</sup> Thus conventional techniques<sup>27, 38, 39</sup> are not applicable. The complete density of (4.12) is not investigated here but in order to illustrate the nature of the test statistic, the present section will obtain the exact density of a gaussian inner product. Such a density is not without utility, since it represents the test statistic density computed for a single receiving element system. The density will be evaluated in terms of the eigenvalues and eigenfunctions of the incident processes and the filtering of the frequency filtering sections. The Karhunen-Loève expansion will be used extensively.

Let  $r(t)$  given by (4.8) be such that

$$\lambda_{r_i} \psi_i(t) = \int_{T_i}^{T_f} K_r(t, u) \psi_i(u) du \quad (4.13)$$

where  $\lambda_{r_i}$  is the  $i$ th eigenvalue of the process  $r(t)$ .

The inner product  $L_n$  is

$$L_n = \underline{r}^T \underline{z} \quad (4.14)$$

where  $\underline{r}$ ,  $\underline{z}$  are gaussian and zero mean, as in the process model taken in Chapter II. Since the  $n$ -dimensional vectors are expanded using the K-L expansion, the co-ordinates of each vector are independent, while

there is correlation between the elements of  $\underline{r}$  and of  $\underline{z}$ . This is represented

$$E[r_i r_j] = E[z_i z_j] = \begin{cases} 0 & i \neq j \\ \neq 0 & i = j \end{cases}$$

$$E[r_i z_j] = \begin{cases} 0 & i \neq j \\ \neq 0 & i = j \end{cases}$$

Using this property of independent co-ordinates, the joint density function of the vectors  $\underline{r}$ ,  $\underline{z}$  is given by

$$p(\underline{r}, \underline{z}) = \prod_{i=1}^n p(r_i, z_i) \quad (4.15)$$

where

$$p(r_i, z_i) = (2\pi)^{-1} |\Lambda_i|^{-1/2} \exp\left(-\frac{1}{2} ([r_i, z_i] \Lambda_i^{-1} [r_i, z_i]^T)\right) \quad (4.16)$$

where

$$\Lambda_i \triangleq E \left[ \begin{bmatrix} r_i \\ z_i \end{bmatrix} \begin{bmatrix} r_i & z_i \end{bmatrix} \right] = \begin{bmatrix} E[r_i^2] & E[r_i z_i] \\ E[r_i z_i] & E[z_i^2] \end{bmatrix} \quad (4.17)$$

and

$$\Lambda_i^{-1} \triangleq W_i \quad (4.18)$$

The joint density can be rewritten as

$$p(\underline{r}, \underline{z}) = \prod_{i=1}^n \frac{1}{(2\pi)} |\Lambda_i|^{-1/2} \exp\left(-\frac{1}{2} (W_{11} r_i^2 + 2W_{12} r_i z_i + W_{22} z_i^2)\right)$$

For stationary processes  $\Lambda_i = \Lambda_j$  all  $i, j$

Thus

$$p(\underline{r}, \underline{z}) = \left(\frac{1}{2\pi}\right)^n |\Lambda|^{-n/2} \exp\left(-\frac{1}{2} (W_{11} \sum_{i=1}^n r_i^2 + 2W_{12} \sum_{i=1}^n r_i z_i + W_{22} \sum_{i=1}^n z_i^2)\right)$$

is the joint density of the  $\underline{r}$ ,  $\underline{z}$  vectors. The exponential summations can be redefined as

$$\sum_{i=1}^n r_i^2 = X^2, \quad \sum_{i=1}^n z_i^2 = Y^2, \quad \sum_{i=1}^n r_i z_i = \underline{r}^T \underline{z} = L_n$$

Thus

$$p(\underline{r}, \underline{z}) = (2\pi)^{-n} |\Lambda|^{-\frac{n}{2}} \exp\left(-\frac{1}{2}(W_{11} X^2 + 2W_{12} \underline{r}^T \underline{z} + W_{22} Y^2)\right)$$

Following the procedure of Miller,<sup>39</sup> generalized spherical co-ordinates for the  $\underline{r}$ ,  $\underline{z}$  variables are introduced, and manipulated to give the marginal frequency function in  $X$ ,  $Y$ ,  $\varphi$  for the definition

$$\underline{r}^T \underline{z} = XY \cos \varphi \quad 0 \leq \varphi \leq \pi$$

giving

$$F(X, Y, \varphi) = \frac{(XY) (XY \sin \varphi)^{n-2} e^{-\frac{1}{2}(W_{11} X^2 + W_{22} Y^2)} e^{-W_{12} XY \cos \varphi}}{2^{n-2} |\Lambda|^{\frac{n}{2}} \Gamma(\frac{1}{2}n) \Gamma(\frac{n-1}{2}) \Gamma(\frac{1}{2})} \quad (4.20)$$

Integrating (4.20) over the range of the new variables

$$L_n = XY \cos \varphi$$

$$\xi = XY \sin \varphi \quad 0 \leq \xi < \infty$$

$$\alpha = X \quad 0 \leq \alpha < \infty$$

$$J = \frac{1}{\alpha \sqrt{L_n^2 + \xi^2}}, \quad \text{the Jacobian, gives}$$

$$p(L_n) = \int_0^\infty \int_0^\infty f(X, Y, \varphi) J \, d\alpha \, d\xi \quad (4.21)$$

With  $K_\nu(\cdot)$  the modified Bessel function of the second kind and order  $\nu$ , the density of  $L_n$  for  $n$  co-ordinates in the expansion is

$$p(L_n) = \frac{|L_n|^{\frac{n-1}{2}} e^{-W_{12} L_n}}{\sqrt{\pi} \Gamma(\frac{1}{2}n) 2^{\frac{n-1}{2}} |\Lambda|^{\frac{1}{2}} (\lambda_{11} \lambda_{22})^{\frac{n-1}{4}} \frac{k_{\frac{n-1}{2}}(|L_n| \sqrt{W_{11} W_{22}})}{2}} \quad (4.22)$$

The matrix  $\Lambda$  is found from (4.17) and (4.18) in terms of the space-time correlation properties of the incident processes, array steering and filtering.

$$E[r_1 r_1] = \int_{T_i}^{T_f} \int_{T_i}^{T_f} K_r(t, u) \psi_i(t) \psi_i(u) \, dt \, du$$

$$E[r_i z_i] = E[z_i r_i] = \int_{T_i}^{T_f} \int_{T_i}^{T_f} \int_{T_i}^{T_f} K_r(t, v) M_\Delta(v, u) \psi_i(t) \psi_i(u) \, du \, dt \, dv$$

$$E[z_1^2] = \int_{T_i}^{T_f} \int_{T_i}^{T_f} \int_{T_i}^{T_f} \int_{T_i}^{T_f} K_r(v, w) M_\Delta(t, v) M_\Delta(w, u) \psi_i(t) \psi_i(u) \, dv \, dw \, dt \, du \quad (4.23)$$

In terms of frequency spectra using integrated transforms

$$E[r_i^2] = \int_{-\infty}^{\infty} S_r(\omega) |\psi_i(j\omega)|^2 \frac{d\omega}{2\pi}$$

$$E[r_i z_i] = E[z_i r_i] = \int_{-\infty}^{\infty} S_r(\omega) M_\Delta(\omega) |\psi_i(j\omega)|^2 \frac{d\omega}{2\pi}$$

$$E[z_i^2] = \int_{-\infty}^{\infty} S_r(\omega) |M_{\Delta}(\omega)|^2 |\psi_i(j\omega)|^2 \frac{d\omega}{2\pi}$$

where

$$\psi_i(j\omega) \triangleq \int_{T_i}^{T_f} \psi_i(t) e^{-j\omega t} dt$$

Thus the density is dependent upon the space-time structure of the incident signal and noise processes in the above manner. The density given in (4.21) with (4.23) can be written under each hypothesis by appropriate substitution of (2.19), (2.20) into the correlation function in equations (4.23).

In summary, the continuous density of  $L$  under either hypothesis is found by obtaining the limit of the density of  $L_n$  as  $n$  grows without bound. An approximation can be realized by truncating the infinite series at  $n$  and using  $n$  co-ordinates. The density given above is the density of a single inner product. The true density must be found for the sum of  $K^2$  such products. Since each of the inner products is non-gaussian and not independent, the analytical effort is not very tractable and has not been investigated here. The density of the single inner product shows the nature of the test statistic  $L$ , and in a following section the sum of many such products is allowed to converge to the gaussian distribution, thus allowing system performance to be expressed analytically. The next section of this paper obtains the true mean and variance of the complete continuous test statistic.

#### 4-2. Calculation of True Mean and True Variance of L

The true first and true second order moments of L (mean and variance) under each hypothesis can be found by direct application of the expectation operator to the decision equation. Under  $H_1$  the received vector  $\underline{r}(t)$  is taken to be

$$\underline{r}(t) = \underline{z}(t) + \underline{n}(t)$$

Thus taking the expected value, the mean of equation (3.10) under  $H_1$  is

$$E[L|H_1] = E \left[ \int_{T_i}^{T_f} \underline{r}^T(t) \underline{M}_{\Delta}(t, u) \underline{r}(u) dt du \right] \quad (4.24)$$

and since the integrand of (4.24) is a Hermitian quadratic form of the form  $\underline{R}^T \underline{Q} \underline{R}$ , the form can be rewritten as<sup>40</sup>

$$\underline{R}^T \underline{Q} \underline{R} = \text{Tr}[\underline{Q} \underline{R} \underline{R}^T] \quad (4.25)$$

where  $\text{Tr}$  is the trace operator.

Thus (4.24) becomes, after commuting the expectation,

$$\begin{aligned} E[L|H_1] &= \text{Tr} \int_{T_i}^{T_f} \underline{M}_{\Delta}(t, u) E[\underline{r}(t) \underline{r}^T(u)] dt du \\ &= \text{Tr} \int_{T_i}^{T_f} \underline{M}_{\Delta}(t, u) \underline{K}_1(t, u) dt du \end{aligned} \quad (4.26)$$

with

$$\underline{K}_1(t, u) = \underline{K}_z(t, u) + \underline{K}_n(t, u)$$

In a similar manner the expected value of  $L$  under  $H_0$  is found

$$E[L|H_0] = \text{Tr} \int_{T_i}^{T_f} \underline{M}_{\Delta}(t, u) \underline{K}_{\underline{n}}(t, u) dt du \quad (4.27)$$

The variance of the test statistic is found from the definition of the variance.

$$\text{Var}[L|H_i] = E[L^2|H_i] - E^2[L|H_i] \quad (4.28)$$

Squaring (3.18) to find the mean-square of  $L$  under  $H_i$

$$L^2 = \int_{T_i}^{T_f} \int_{T_i}^{T_f} \underline{r}^T(t) \underline{M}_{\Delta}(t, u) \underline{r}(u) \underline{r}^T(x) \underline{M}_{\Delta}(x, y) dt du dx dy \quad (4.29)$$

and applying property (4.25) and the property that matrix products commute under the trace operator<sup>40</sup>

$$\text{Tr}(ABC) = \text{Tr}[\text{any order}]$$

gives

$$L^2 = \int_{T_i}^{T_f} \dots \int_{T_i} \text{Tr}[\underline{M}_{\Delta}(t, u) \underline{M}_{\Delta}(x, y) [\underline{r}(t) \underline{r}^T(u) \underline{r}(x) \underline{r}^T(y)]] dx dy dt du$$

Applying the expectation under  $H_i$  and the expectation theorem for the product of gaussian variables<sup>33, 26</sup> it follows that

$$E[L^2|H_i] = 2 \text{Tr} \int_{T_i}^{T_f} \int_{T_i}^{T_f} \underline{M}_{\Delta}(t, u) \underline{K}_{\underline{i}}(u, x) \underline{M}_{\Delta}(x, y) \underline{K}_{\underline{i}}(y, t) dt du dx dy \quad (4.30)$$

$$+ \text{Tr} \int_{T_i}^{T_f} \int_{T_i}^{T_f} \underline{M}_{\Delta}(t, u) \underline{K}_{\underline{i}}(t, u) \underline{M}_{\Delta}(x, y) \underline{K}_{\underline{i}}(x, y) dt du dx dy$$

The second set of integrals in (4.30) is the  $E^2[L|H_i]$  which, when taken with (4.29) gives

$$\text{Var}[L|H_i] = 2\text{Tr} \int_{T_i}^{T_f} \int \int \int M_{\underline{\Delta}}(t, u) K_{\underline{i}}(u, x) M_{\underline{\Delta}}(x, y) K_{\underline{i}}(y, t) dt du dx dy \quad (4.31)$$

Thus the true mean and true variance under each hypothesis are given by equations (4.27, 31). These equations give, in general, the first and second moments for both stationary and non-stationary processes. If  $\{r(t)\}$  is a stationary process, the equations (4.27, 31) can be written, using integrated transforms,<sup>14, 34, 35</sup> and Parseval's theorem<sup>14</sup> in terms of the process power spectra.

$$E[L|H_i] = \int S_{\underline{i}}^{-1}(\omega) S_{\underline{z}}(\omega) S_{\underline{n}}^{-1}(\omega) S_{\underline{i}}(\omega) \frac{d\omega}{2\pi} \quad (4.32)$$

and

$$\text{Var}[L|H_i] = 2\text{Tr} \int_{-\infty}^{\infty} |S_{\underline{i}}^{-1}(\omega) S_{\underline{z}}(\omega) S_{\underline{n}}^{-1}(\omega) S_{\underline{i}}(\omega)|^2 \frac{d\omega}{2\pi} \quad (4.33)$$

The above equations for the true mean and variance of L under each hypothesis will be used extensively in the gaussian approximation to the true density that follows and in evaluating system performance.

#### 4-3. Gaussian Approximation for the Test Statistic Distribution

The density of the single element test statistic, L under either hypothesis was given by equation (4.22) As can be seen, this density is quite complicated and difficult to manipulate analytically to obtain exact system performance. Such difficulty can be overcome, however, by the

the use of an approximation to the exact density. One such approximation is a truncation of the infinite series in (4.22) and the use of numerical techniques to obtain system performance. Another approach is a direct approximation of the true density by substitution of a gaussian density for (4.22). In this approximation  $L$  is taken to be a gaussian variable with mean given by the true mean of  $L$  (computed in (4.27, 28) and with variance given by the true variance of  $L$  (computed in (4.31)).

Justification for this approximation can be seen by noting that the test statistic  $L$  was found in IV-2 to be a  $k$ th order inner product, and as such is the summation of  $K^2$  non-gaussian  $\chi^2$  variables.<sup>27, 40, 41</sup> It is known that the density of a summation of non-gaussian independent variables converges to the gaussian distribution quite rapidly through the properties of the Central Limit Theorem.<sup>27, 38</sup> This convergence is most rapid in the vicinity of the mean of the density. Price<sup>8, 36</sup>, Green<sup>36</sup>, and Middleton<sup>42</sup> have investigated the gaussian approximation quite extensively and have shown its validity in computing system performance.

The gaussian approximation for the test statistic has been investigated for the "threshold" or coherently undetectable case by Middleton<sup>42</sup> and Price<sup>36</sup>. Their studies have shown that the approximation yields useful results for cases in which the signal-to-noise ratio (SNR) is low. If a large average signal power is available, implying high SNR, system detection requirements are usually not critical.

However, for low SNR the effects of array and incident process spatio-temporal correlation properties become important, since it is usually necessary to attain nearly optimum system configuration and performance, in order to meet system detection capability specifications. The gaussian approximation furnishes performance analysis methods for such cases of low SNR. Thus the approximation is most valid where it is of greatest utility. Helstrom has examined another approximation to (4.22) using the Gram-Charlier series expansion and found comparable results.

Thus the density in (4.22) can be approximated as gaussian with mean given by (4.27, 28) and variance by (4.31). The following system performance criteria analysis and subsequent case studies employ the gaussian approximation of the test statistics.

With the density of  $L$  gaussian, the error probabilities of the system can be defined by

$$\begin{aligned} \text{prob. false alarm} = P_F &\triangleq \int_{\gamma}^{\infty} p(L|H_0) dL \\ &= \text{erfc} \left( \frac{\ln \eta}{\delta_0} + \frac{\delta_0}{2} \right) \end{aligned}$$

where  $\gamma$  is the threshold, and similarly

$$\begin{aligned} \text{prob. of miss} = P_M &\triangleq \int_{-\infty}^y p(L|H_1) dL \\ &= \text{erf}\left(\frac{\ln \eta}{\delta_0} - \frac{\delta_0}{2}\right) \end{aligned} \quad (4.35)$$

$$\text{where } \text{erf}(x) \triangleq \frac{1}{\sqrt{2\pi}} \int_{-\infty}^x \exp\left(-\frac{x^2}{2}\right) dx$$

$$\text{erfc}(x) \triangleq 1 - \text{erf}(x)$$

$P_D$ , the probability of detection, is defined as

$$P_D \triangleq 1 - P_M = \text{erfc}\left(\frac{\ln \eta}{\delta_0} - \frac{\delta_0}{2}\right)$$

The parameter  $\delta_0$  is related to the output signal to noise ratio by

$$\delta_0 = \text{SNR}_0$$

where

$$(\text{SNR}_0)^2 \triangleq \frac{(E[L|H_1] - E[L|H_0])^2}{(\text{Var}[L|H_1] \text{Var}[L|H_0])^{1/2}} = \delta_0^2 \quad (4.36)$$

The validity of this measure of system performance has been found by Price<sup>8</sup>. The numerator of the  $\delta_0^2$  parameter is a measure of the distance between the means of the densities under each hypothesis, while the denominator is a measure of the variance or spread of the densities. Thus, system performance will be enhanced by increasing the distance between the means, and degraded by an increasing variance.

The  $\delta_o^2$  parameter will be used as measure of system performance in the remainder of this paper.

Using equation (4.36) for  $\delta_o^2$  and equations (4.27), (4.28), (4.31) for the parameters in (4.36), the performance characteristics can be written in general as<sup>14</sup>

$$\delta_o^2 = \frac{\left[ \text{Tr} \int_{T_i}^{T_f} \underline{M}_{\Delta}(t, u) \underline{K}_{\Sigma}(t, u) dt du \right]^2}{2 \left( \int_{T_i}^{T_f} \int_{\dots} \underline{M}_{\Delta}(t, u) \underline{K}_{\underline{1}}(u, x) \underline{M}_{\Delta}(x, y) \underline{K}_{\underline{1}}(y, t) dt du dx dy \right) \times \left( \int_{T_i}^{T_f} \int_{\dots} \underline{M}_{\Delta}(t, u) \underline{K}_{\underline{0}}(u, x) \underline{M}_{\Delta}(x, y) \underline{K}_{\underline{0}}(y, t) dt du dx dy \right)} \quad (4.37)$$

The parameter  $\delta_o^2$  reflects the dependence of system performance upon spatio-temporal structure of the incident processes, array geometry and steering, signal-to-noise power ratio, and temporal filtering and combining techniques. Equation (4.37) is the general expression for the receiver performance for both stationary and non-stationary processes. If the incident processes are stationary as defined previously, new insight into the nature of  $\delta_o^2$  is found.

With stationarity and binary hypothesis  $\delta_o^2$  can be written in terms of the power spectra of the incident processes, filtering requirements and steering delays as

$$\delta_o^2 = \frac{1}{2} \frac{\left( \text{Tr} \int_{-\infty}^{\infty} \underline{S}_{\underline{Q}}(\omega) \underline{S}_{\underline{Z}}(\omega) \frac{d\omega}{2\pi} \right)^2}{\left( \text{Tr} \int_{-\infty}^{\infty} |\underline{S}_{\underline{Q}}(\omega) \underline{S}_{\underline{I}}(\omega)|^2 \frac{d\omega}{2\pi} \text{Tr} \int_{-\infty}^{\infty} |\underline{S}_{\underline{Q}}(\omega) \underline{S}_{\underline{n}}(\omega)|^2 \frac{d\omega}{2\pi} \right)^{1/2}} \quad (4.38)$$

The above expression may be used to obtain system performance curves for detection of stationary random signals. Further simplification of (4.38) can be found for the threshold or "coherently undetectable" case.<sup>8, 14, 36</sup>

#### 4.4 Threshold Performance

The performance index given by (4.38) for stationary processes can be further simplified for the "threshold" or "coherently undetectable" case. Much of this analysis was first investigated by Middleton<sup>42</sup> and Price<sup>8, 36</sup>.

The assumption that is made in the threshold case is that the signal-to-noise-ratio is low, or that the magnitude of the elements of the noise spectral matrix are much larger than the corresponding elements in the signal spectral matrix. Mathematically, this is stated as

$$S_{n_{ij}}(\omega) \gg S_{z_{ij}}(\omega) \quad \text{all } i, j$$

In such a case

$$\underline{S}_{\underline{I}}(\omega) = \underline{S}_{\underline{Z}}(\omega) + \underline{S}_{\underline{I}}(\omega) \approx \underline{S}_{\underline{n}}(\omega)$$

and

$$\begin{aligned} \underline{S}_Q(\omega) &= \underline{S}_1^{-1}(\omega) \underline{S}_z(\omega) \underline{S}_n^{-1}(\omega) \\ &\approx \underline{S}_n^{-1}(\omega) \underline{S}_z(\omega) \underline{S}_n^{-1}(\omega) \end{aligned}$$

Using these relations in (4.38) and noting that  $\text{Var}[L|H_0] \approx \text{Var}[L|H_1]$

gives

$$\begin{aligned} \delta_o^2 &= \frac{1}{2} \frac{(\text{E}[L|H_1] - \text{E}[L|H_0])^2}{\text{Var}[L|H_0]} \\ &= \frac{1}{2} \text{Tr} \int_{-\infty}^{\infty} \underline{S}_n(\omega) \underline{S}_z(\omega) \underline{S}_n^{-1}(\omega) \underline{S}_z(\omega) \frac{d\omega}{2\pi} \end{aligned}$$

for a steered array  $\underline{S}_z(\omega) = \underline{S}_{z'}(\omega)$  is given by (3.32) and  $\underline{S}_n(\omega) = \underline{S}_{n'}(\omega)$

by (3.33). Thus

$$\delta_o^2 = \text{Tr} \int_{-\infty}^{\infty} \underline{S}_{n'}^{-1}(\omega) \underline{1}\underline{1}^T \underline{S}_{n'}^{-1}(\omega) \underline{1}\underline{1}^T \underline{S}_{z'}^2(\omega) \frac{d\omega}{2\pi} \quad (4.39)$$

and

$$\begin{aligned} \underline{S}_{n'}^{-1}(\omega) \underline{1}\underline{1}^T &= \left[ \sum_j^K S_{n'}^{ij}(\omega) \right] \\ \text{Tr} \left[ (\underline{S}_{n'}^{-1}(\omega) \underline{1}\underline{1}^T)^2 \right] &= \left( \sum_i^K \sum_i^K S_{n'}^{ij}(\omega) \right)^2 \end{aligned} \quad (4.40)$$

Substitution of (4.40) into (4.39) and taking the trace operator inside

the integral gives

$$\delta_o^2 = \int_{-\infty}^{\infty} \left( \underline{S}_z(\omega) \sum_{i=1}^K \sum_{j=1}^K S_{n'}^{ij}(\omega) \right)^2 \frac{d\omega}{2\pi} \quad (4.41)$$

Equation (4.41) is one final result for the system performance index  $\delta_o^2$ . The index is expressed in terms of the input signal spectrum  $S_z(\omega)$ , which may have a multipath representation, and the steered noise matrix. The latter contains the effects of array geometry, array steering, and spatio-temporal correlation properties of the incident processes as well as system interference. The elements  $S_{n,ij}(\omega)$  can be found from equation (2.18). Using these results, one can calculate the index  $\delta_o^2$  for various values of array steering and geometry, as well as different space-time properties of both the signal and noise fields. Using  $\delta_o^2$  one can then obtain the receiver-operating-characteristics (ROC) curves to specify system performance in terms of error probabilities. Using these curves, the designer can establish the effects upon system performance of various parameters in the system, such as the effects of the number of array elements, various array geometrics, multipath structure, and of the cross element space-time correlation properties which are related to the array steering and incident process structure by equations (2.13) and (2.18).

The previous chapter developed the optimum decision equations for the array detection of random signals in noise. Interpretation yielded a number of system configurations (both stationary and time-varying). The performance of these optimum systems was then investigated for both the general case and the single signal (steered array)

stationary process case. Introduction of the threshold assumption allowed further simplification of the performance index and interpretation to illustrate the effects of steering and cross link properties of the random fields. The following section will investigate, as a case studies, the performance of the optimum systems to determine the effects of array geometry (element spacing and position), the effects of multipath in the incident signal processes, and the effects of cross-element correlation properties of the random fields. Analysis and interpretation of the resulting performance curves (ROC) will establish guidelines as to techniques for enhancing system performance, by valid physical consideration.

## CHAPTER V

### CASE STUDY

Using the results of Chapters III, IV, and the model of Chapter II, the following chapter analyzes in detail the performance of the previously derived system configurations for various cases.

The first case study will investigate the detection performance of the single element optimum receiving system configuration. The incident processes will be assumed gaussian, with the signal portion of the received process consisting of a two path, correlated-multipath random process with "Markovian" correlation function. The system performance is evaluated in terms of the effects produced by the delay between the multipaths, and the division of signal power between the two resolvable paths, thus establishing the effects of the multipath structure upon single receiving element system performance.

The second case study will employ a two element receiving array. In this study the effects of multipath structure upon system performance will again be established. In addition, the effects of element geometry and cross-link spatio-temporal correlation properties of the incident random processes will be pinpointed. The physical aspects, multipath effects, element geometry, and noise correlation properties will then be combined, illustrating a method for enhancing system performance by proper selection of array geometry.

Finally, using the "best" geometry found in the second case study, the effects of the number of array elements, upon performance, will be illustrated.

Thus, these case studies establish the performance characteristics of single and multiple element receiver systems. They illustrate variations in system performance due to multipath structure in the random signals, array geometry, array steering, and space-time correlation properties of the incident random processes. In general, the case studies establish the role of spatio-temporal correlation properties of the incident processes, in terms of coupling by the array receiving system, for the random, multipath signal and noise environment.

#### 5-1. Homogeneous Interference Assumption

The steered noise spectral matrix was given by equation (3.33). If the noise spectrum at each receiving element is assumed to be the same, the noise interference field is said to be a homogeneous field. Such a space-time structure of the noise field is frequently encountered in both the sonar and radar cases, as well as in seismology.<sup>1,11,14</sup> The homogeneity of the noise is represented mathematically by

$$S_{n'_{ij}}(\omega) = S_{n'_{ij}}(\omega) \quad \text{all } i, j$$

In addition, it is assumed that there is some common factorable noise spectral property in the elements of the noise spectral matrix.

Thus, equation (3.33) can be written as

$$\underline{S}_{n'}(\omega) = \underline{S}_n(\omega) \underline{\xi}(\omega) \quad (5.1)$$

where the  $\underline{\xi}(\omega)$  matrix has elements

$$\varphi_{ij}(\omega) = \frac{S_{n'ij}(\omega)}{S_n(\omega)} \quad (5.2)$$

Substitution of the above equations into the threshold detection performance index, (3.39), gives the new index

$$\begin{aligned} \delta_o^2 &= \text{Tr} \int_{-\infty}^{\infty} \left( \frac{S_z(\omega)}{S_n(\omega)} \underline{\xi}^{-1}(\omega) \underline{11}^T \right)^2 \frac{d\omega}{2\pi} \\ &= \int_{-\infty}^{\infty} \left( \frac{S_z(\omega)}{S_n(\omega)} \right)^2 \left( \sum_{i=1}^K \sum_{j=1}^K \varphi^{ij}(\omega) \right)^2 \frac{d\omega}{2\pi} \end{aligned} \quad (5.3)$$

Defining

$$\frac{S_z(\omega)}{S_n(\omega)} \triangleq \Gamma_o(\omega) = \text{signal-noise-ratio-function}$$

and the array gain function

$$\sum_{i=1}^K \sum_{j=1}^K \varphi^{ij}(\omega) \triangleq G_o(\omega) = \text{array gain function} \quad (5.4)$$

one can write the performance index as

$$\delta_o^2 = \int_{-\infty}^{\infty} \Gamma_o^2(\omega) G_o^2(\omega) \frac{d\omega}{2\pi} \quad (5.5)$$

It is seen from equation (5.5) that the performance is a function of the input signal-to-noise ratio and an array gain function which contains

the enhancement due to the steering, frequency filtering, and combining as well as the coupling produced by the array. It is the index in (5.5) that is employed to analyze the following case studies.

5-2. Case I - Single Element in Random Multipath Environment - Single Plane Wave Coherently Undetectable Case

For the first case study, the receiver consists of a single receiving element. The system decision equation (3.18) for detection of the random stationary signal  $z(t)$  becomes

$$L = \int_{-\infty}^{\infty} R^*(\omega) S_Q(\omega) R(\omega) \frac{d\omega}{2\pi} \quad (5.6)$$

with the filter  $S_Q(\omega)$  given by

$$S_Q(\omega) = \frac{S_z(\omega)}{S_n(\omega)[S_z(\omega) + S_n(\omega)]}$$

The portion of  $S_Q(\omega)$ ,  $[S_z(\omega)/S_n(\omega)]$  is recognized as the "Wiener" estimation filter.<sup>43, 14</sup>

This system configuration is shown in the figure, 5-1, with the signal spectrum  $S_z(\omega)$  being found below. The performance of the system is found from (5.3), where the array gain equals 1 and  $S_{n'}(\omega) = S_n(\omega)$ .

The performance index is

$$\delta_o^2 = \int_{-\infty}^{\infty} \left( \frac{S_z(\omega)}{S_n(\omega)} \right)^2 \frac{d\omega}{2\pi} \quad (5.7)$$

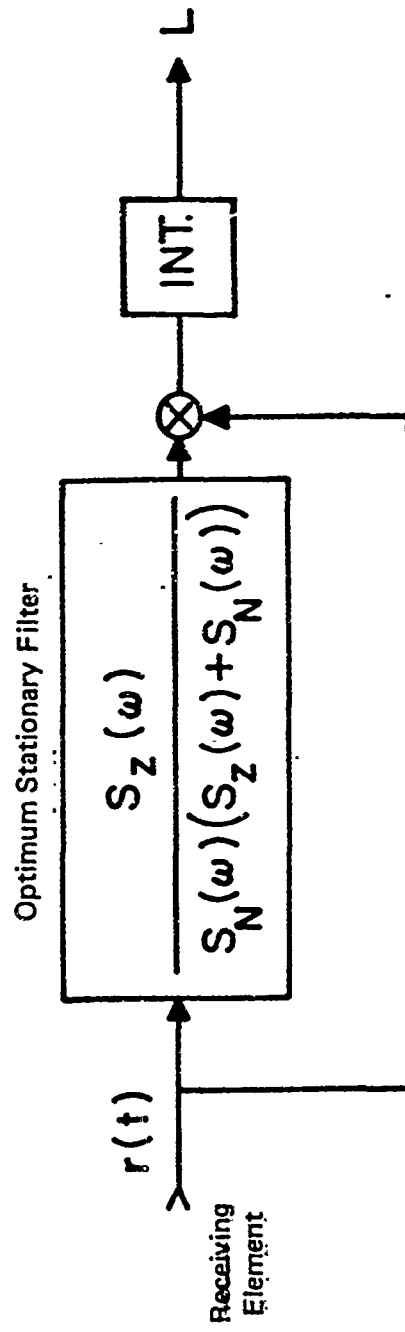


Figure 5-1. Single Receiving Element Receiver Structure

Assuming the random signal to have a two path structure with  $\frac{A\%}{100}$  of the signal field in the first path and  $\frac{B\%}{100}$  in the second path with delay between the paths,  $\Delta$ . Mathematically the signal is represented

$$z(t) = z_1(t) + z_2(t)$$

where  $z_1(t) = Az(t)$  and  $z_2(t)$  is a delayed version of  $z_1(t)$

$$z_2(t) = Bz(t-\Delta)$$

The correlation function of  $z(t)$  is

$$\begin{aligned} K_z(t, u) = E[z(t)z(u)] &= A^2 K_z(t, u) + AB K_z(t, u-\Delta) + AB K_z(t-\Delta, u) \\ &+ B^2 K_z(t-\Delta, u-\Delta) \end{aligned}$$

and for stationary processes,  $t - u = \tau$ , thus

$$K_z(\tau) = (A^2 + B^2) K_z(\tau) + AB [K_z(\tau + \Delta) + K_z(\tau - \Delta)] \quad (5.9)$$

The power spectrum of  $z(t)$  is

$$\begin{aligned} S_z(\omega) = \mathcal{F}\{K_z(\tau)\} &= (A^2 + B^2) S_z(\omega) + AB S_z(\omega) [e^{j\omega\Delta} + e^{-j\omega\Delta}] \\ &= (A^2 + B^2 + 2AB \cos \omega\Delta) S_z(\omega) \end{aligned}$$

Let the random signal correlation be Markovian with single pole spectrum given by

$$S_z(\omega) = \frac{2\omega_c P_z}{\omega_c^2 + \omega^2} \quad (5.10)$$

where  $\omega_c$  is the 3 dB bandwidth of the random signal process and  $P_z$  is the average power. Thus  $S_z(\omega)$  in (5.6) and (5.7) is

$$S_z(\omega) = (A^2 + B^2 + 2AB\cos\omega\Delta) \frac{2\omega_c P_z}{\omega_c^2 + \omega^2} \quad (5.11)$$

The system performance index is

$$\delta_o^2 = \int_{-\infty}^{\infty} \left( \frac{(A^2 + B^2 + 2AB\cos\omega\Delta) 2\omega_c P_z}{\omega_c^2 + \omega^2} \right)^2 \frac{d\omega}{2\pi} \quad (5.12)$$

A plot of the effective signal-noise-ratio,  $\delta_o$ /SNR, versus the normalized % of power in the second path is shown in figure 5-2 for various values of multipath delay.

The plot shows that performance

1. degrades as the multipath delay,  $\Delta$ , increases
2. degrades as a larger portion of the signal power is transmitted via the second path.

The limiting curve of "worst performance" is the curve  $\Delta \rightarrow \infty$ , while the "best performance" is for  $\Delta = 0$ , implying no multipath structure.

The physical effect of the multipath structure is to distribute the signal energy over a larger amount of time. This can be seen by assuming that during the signal band,  $T_f - T_i = T$ , for no multipath,  $E$ , a fixed amount of energy is transmitted. The signal energy per time unit, available to the receiver is  $\frac{E}{T}$  and the input signal-to-noise ratio,

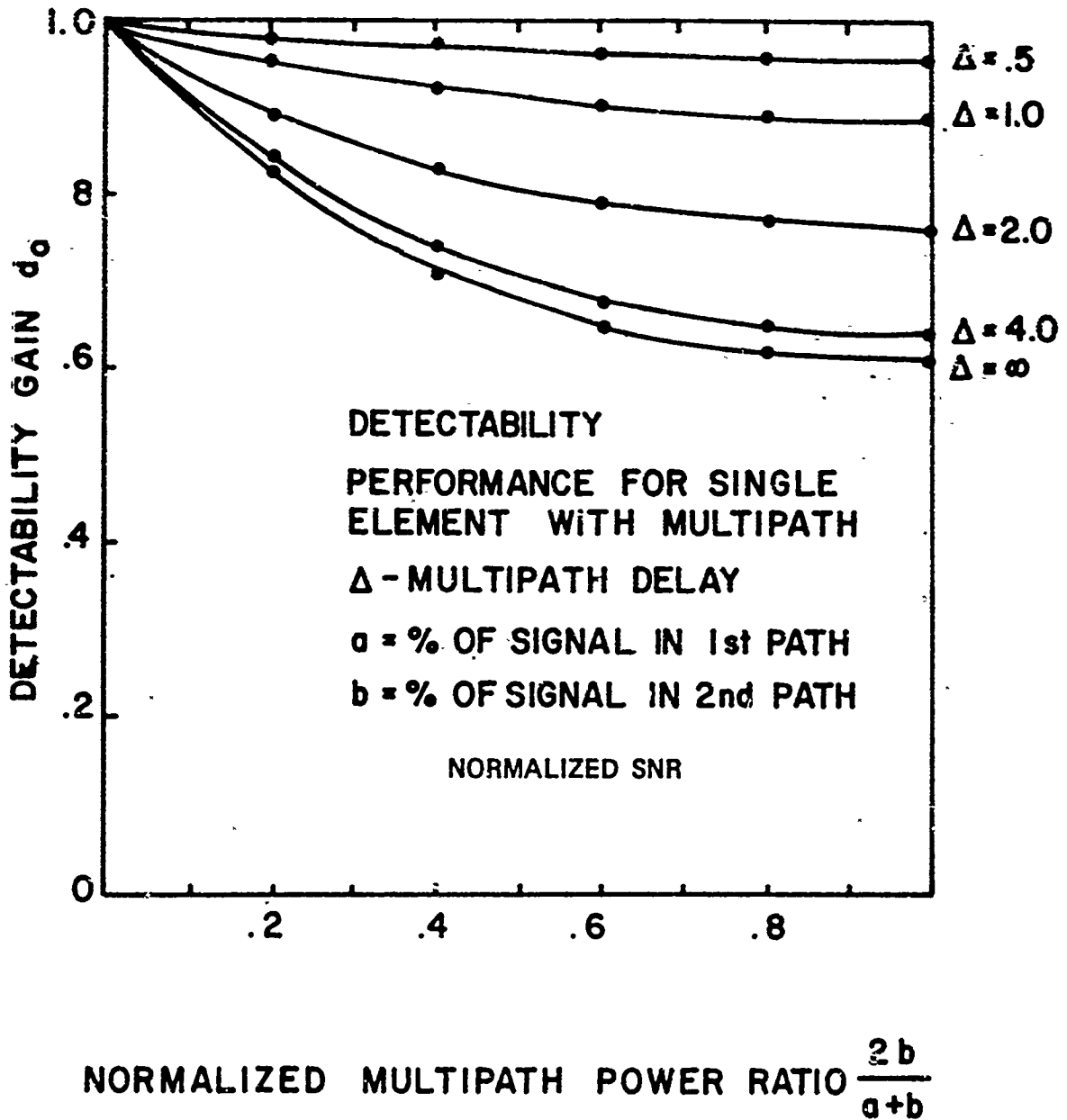


Figure 5-2

with  $N_p$  representing the noise power is

$$\text{SNR}_I = \frac{E}{TN_p}$$

If two paths exist with A% of the energy transmitted via the first path and B% transmitted via path two at time  $\Delta$ , the total energy available is still E, since  $A+B=1$ , but the time interval of total transmission is now  $T+\Delta$ . The input signal-to-noise ratio is lower, shown by

$$\text{SNR}_I = \frac{AE+BE}{(T+\Delta)N} < \frac{E}{TN}$$

The effective SNR given by the performance index (5.12) shows quantitatively the above effects. In figure 5-2, the index decreases due to increasing  $\Delta$ , shown qualitatively above, and is "worst" for  $\Delta \rightarrow \infty$ . Best performance is achieved when  $\Delta$  is small; the signal energy concentration being greatest in the shorter transmission or observation time period.

The degradation due to more equal distribution of energy over the two paths with constant  $\Delta$  is seen by examination of the  $\text{SNR}_I$  for a single path. For A% of E transmitted in the first path during T, and B% in the second, the SNR for each path is

$$\text{SNR}_1 = \frac{AE}{TN}$$

$$\text{SNR}_2 = \frac{BE}{TN}$$

The receiver in effect must process two weaker signals in the presence of constant noise power, rather than a single strong signal. Thus, the effective SNR for each path is lower than for a single path, and the resulting performance degrades. This effect is shown in the figure by the decreasing performance index for increasing power ratio (or increasing energy in the second path). Thus, the performance for a single element receiver is optimum when the multipath structure is such that a majority of the available signal energy is transmitted in a single path. If the power does split appreciably, the best performance occurs for small delay  $\Delta$ .

The performance for the single element receiver and given environment cannot be improved without some influence upon the multipath structure of the information channel. As this is almost always not the case, since the multipath structure is normally a natural phenomenon of the channel and not under the designer's influence, the performance of a single element is almost entirely fixed by the channel, with little improvement capability available. Figure 5-3 shows ROC curves for the single receiver element normalized SNR, and various multipath structures, illustrating the performance variations noted above.

5-3. Case II - Two Element Array, No Multipath - Coherently Undetectable Case

Turning now to the array detection case, the following case study analyzes the performance of a two element array where the

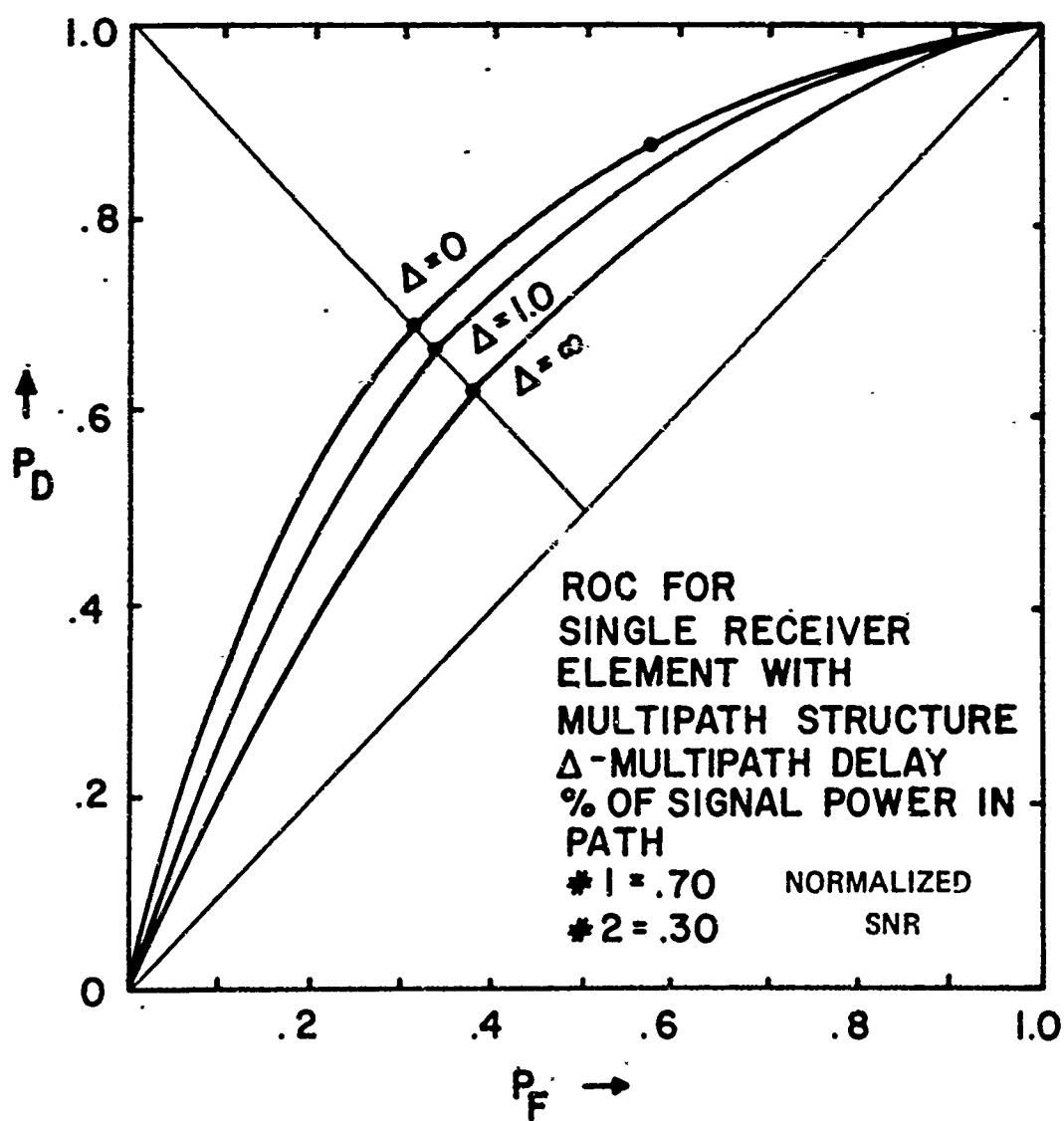


Figure 5-3

random signal has no multipath structure. In this situation the steered signal spectrum matrix (3.32) is

$$\underline{S}_z(\omega) = S_z(\omega) \underline{11}^T$$

The steered noise spectrum matrix is (3.33)

$$\underline{S}_n(\omega) = [S_{n,ij}]$$

The elements  $S_{n,ij}(\omega)$  are given by equation (2.8) and the waveform delay is given by (2.13). Thus

$$\underline{S}_n(\omega) = \begin{bmatrix} S_{n11}(\omega) & S_{n12}(\omega) e^{-j\omega\tau} \\ S_{n21}(\omega) e^{j\omega\tau} & S_{n22}(\omega) \end{bmatrix} \quad (5.13)$$

Application of the homogeneous noise field assumption, and assuming that the correlation properties of the unsteered noise matrix are such that

$$\begin{aligned} S_{n,ij}(\omega) &= S_c(\omega) \quad i = j \\ &= \frac{N_0}{2} + S_c(\omega) \quad i \neq j \end{aligned} \quad (5.14)$$

where  $S_c(\omega)$  is the common link power spectrum, the steered noise matrix is

$$\underline{S}_n(\omega) = \left[ \frac{N_0}{2} + S_c(\omega) \right] \begin{bmatrix} 1 & A e^{-j\omega\tau} \\ A e^{j\omega\tau} & 1 \end{bmatrix} \quad (5.15)$$

where  $A$  is defined

$$A \triangleq \frac{S_c(\omega)}{\frac{N_o}{2} + S_c(\omega)} \quad (5.16)$$

The optimum system configuration in single combiner form is shown in figure 5-4.

Putting equation (5.15) into the form of (5.1) gives the common spectral occupancy  $S_n(\omega)$  and the  $\phi(\omega)$  matrix.

$$S_n(\omega) = \frac{N_o}{2} + S_c(\omega) \quad (5.17)$$

$$\underline{\phi}(\omega) = \begin{bmatrix} 1 & A e^{-j\omega\tau} \\ A e^{j\omega\tau} & 1 \end{bmatrix} \quad (5.18)$$

Finding  $\underline{\phi}^{-1}(\omega)$

$$\underline{\phi}^{-1}(\omega) = \frac{\begin{bmatrix} 1 & -A e^{j\omega\tau} \\ -A e^{-j\omega\tau} & 1 \end{bmatrix}}{1 - A^2} \quad (5.19)$$

and the array gain function (eq. 5-4) becomes

$$G_o(\omega) = \frac{2(1 - A \cos \omega\tau)}{1 - A^2} \quad (5.20)$$

For mathematical simplicity, assume that the noise is entirely white, with  $S_c(\omega) = \frac{N_o}{2}$ ; thus

$$A = \frac{1}{2}, \quad S_n(\omega) = N_o$$

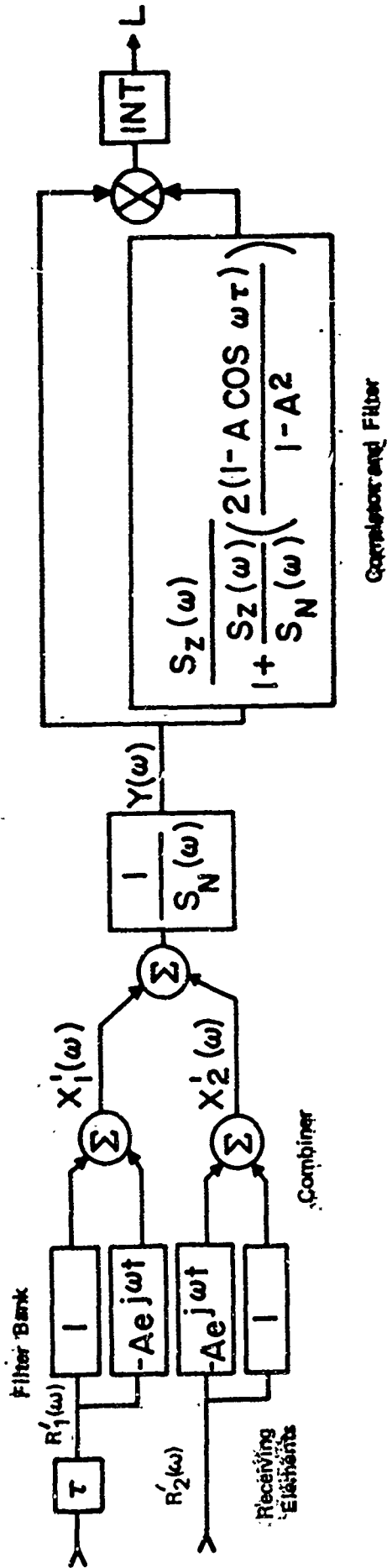


Figure 5-4. Two Element Receiving System Configuration (single combiner)

Substitution of these terms into the performance index equation (5.3) and taking

$$S_z(\omega) = \frac{2\omega_c P_z}{\omega_c^2 + \omega^2}$$

in Case Study I gives

$$\delta_o^2 = \int_{-\infty}^{\infty} \left( \frac{2\omega_c P_z (\omega_c^2 + \omega^2)}{N_o} \right)^2 \left( 1 - \frac{1}{2} \cos \omega \tau \right)^2 \frac{d\omega}{2\pi} \quad (5.21)$$

Integration of (5.21) and plotting the error probabilities for various values of  $\tau$  gives the ROC operating curves given in figure 5-5. These curves show the variation of the system performance with changing element separation, related by equation (2.13). The "best" performance is realized for infinite separation, while "worst" performance results for  $\tau=0$ , (no separation).

The improvement in performance, obtained by making  $\tau$  as large as possible, can be interpreted in terms of the "detectability resolution" of the entire space time receiving system. In antenna design (spatial detection), it is often desirable to make the main lobe of the beam pattern as narrow as possible while simultaneously reducing the side lobes (minor lobes) of the antenna array pattern.<sup>4, 5</sup> These requirements are mutually exclusive, to a certain degree, since narrowing the beam usually results in increased sidelobe level. The problem is usually solved by employing an array of elements spaced and steered

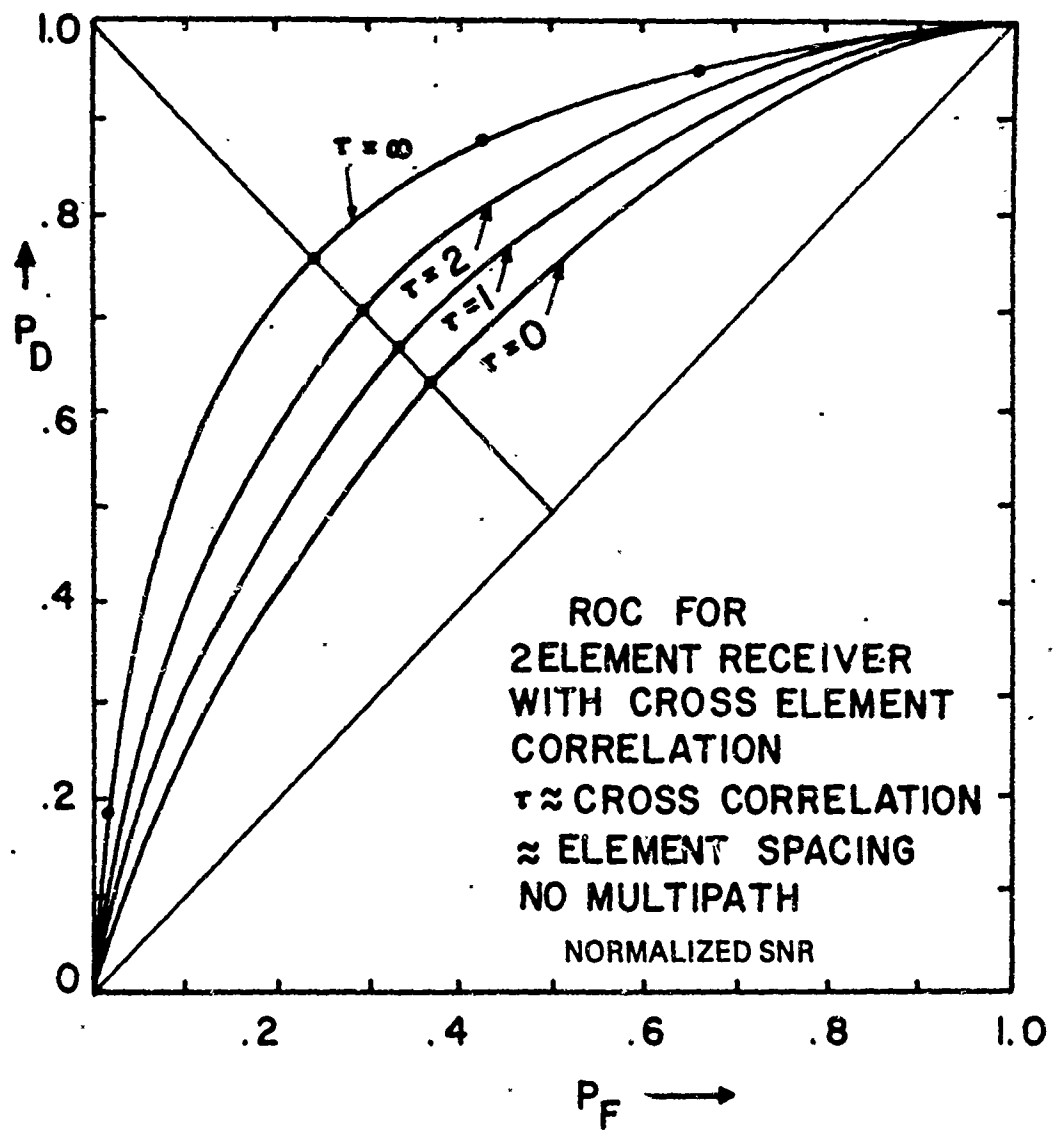


Figure 5-5

to give a narrow directional main beam. The power received by each element is then weighted (shaded) to give a desired sidelobe level.<sup>2, 4, 5</sup>

There are numerous shading schemes to obtain certain sidelobe characteristics.<sup>2, 44, 4, 5</sup> In these methods the physics (space-time) structure of the noise field is not taken into the problem analysis, thus the resulting resolution (detection enhancement) is due to spatial resolution only. It has been found, particularly in the area of radio astronomy<sup>45</sup>, that "best" resolution is achieved by widely spacing the elements of the array. As the element spacing increases, the resolution increases markedly. Multi-element arrays with large element separation, such as in interferometers, are widely employed in much of present day radio astronomy research.<sup>45</sup>

In the case of optimum space-time detection, the analysis includes the effects upon detection capability that arise from consideration of the space-time noise fields as well as the spatial array beam pattern. Here also some of the same characteristics of the receiving systems are wanted: narrow directional main lobe, low sidelobe level, and effective noise field rejection. The latter requirement is added because the array, together with the steering, combiner, and lattice frequency filtering stages, produces effective noise rejection and signal enhancement by adjustment of the sidelobe levels. The noise rejection and signal enhancement result from the optimal system configuration

developed in Chapter III and discussed there. Thus the space-time analysis yields the system detection performance in terms of both the spatial resolution and the filtering (frequency) resolution of the incident processes. The combined effects and resulting performance index can be termed the total array "detectability resolution," combining the disciplines of antenna resolution theory and statistical communications and optimal filtering theory.

The increased performance capability observed in figure 5-5 with increased separation of the elements is thus the result of sidelobe 1) noise rejection due to optimal lattice combining in the frequency filtering stages; 2) narrowing the main lobe (yielding improved spatial resolution) due to increased separation of the elements. The element geometry (separation) and steering produce a spatial beam pattern with a narrow directional main lobe; the optimum frequency filtering and combining stages, dictated by the space-time structure of the incident processes and the array geometry, perform sidelobe rejection and shading, as well as statistically filtering the received data. Increasing the separation produces a narrower, more directional spatial beam pattern, thereby improving resolution in space, and, since the new optimal frequency filtering and combining stages contain the new spatial variables as parameters, these stages produce a new optimal noise rejection and sidelobe level adjustment pattern, effectively yielding

an improved detection capability. The improvement in performance due to element separation can be seen by plotting the beam pattern of the above array receiving system. In figure 5-6 the beam pattern for a two receiving element system is shown for the above interference field and two values of element spacing. The solid curve represents a spacing of  $\lambda/2$ , while the broken curve is the beam pattern for a spacing of  $1.0\lambda$ . As the spacing is increased from  $\lambda/2$  to  $1.0\lambda$ , the beam pattern changes in two ways; the main lobe narrows and the side lobe level increases. The frequency filtering and combining stages will compensate for the increased sidelobe level by producing optimal noise rejection-signal enhancement in frequency, while the narrow main beam will produce improved signal resolution in space. The over-all result is improved detection performance capability. The same results are seen in figure 5-7. Here the beam pattern for the two element system is plotted for two spacings and a signal incident at  $30^\circ$ . The increased spacing gives a narrower main lobe and improved detectability resolution. Therefore, consideration of the detection problem as a combined, integrated, space-time problem, rather than dichotomizing the problem into a spatial (antenna) problem and data processing problem, yields a more concise, broader interpretation of design requirements. The above case study shows that improved system performance is realized for a two element array in a non-multipath environment by making the separation of the receiving elements as large as is physically possible.

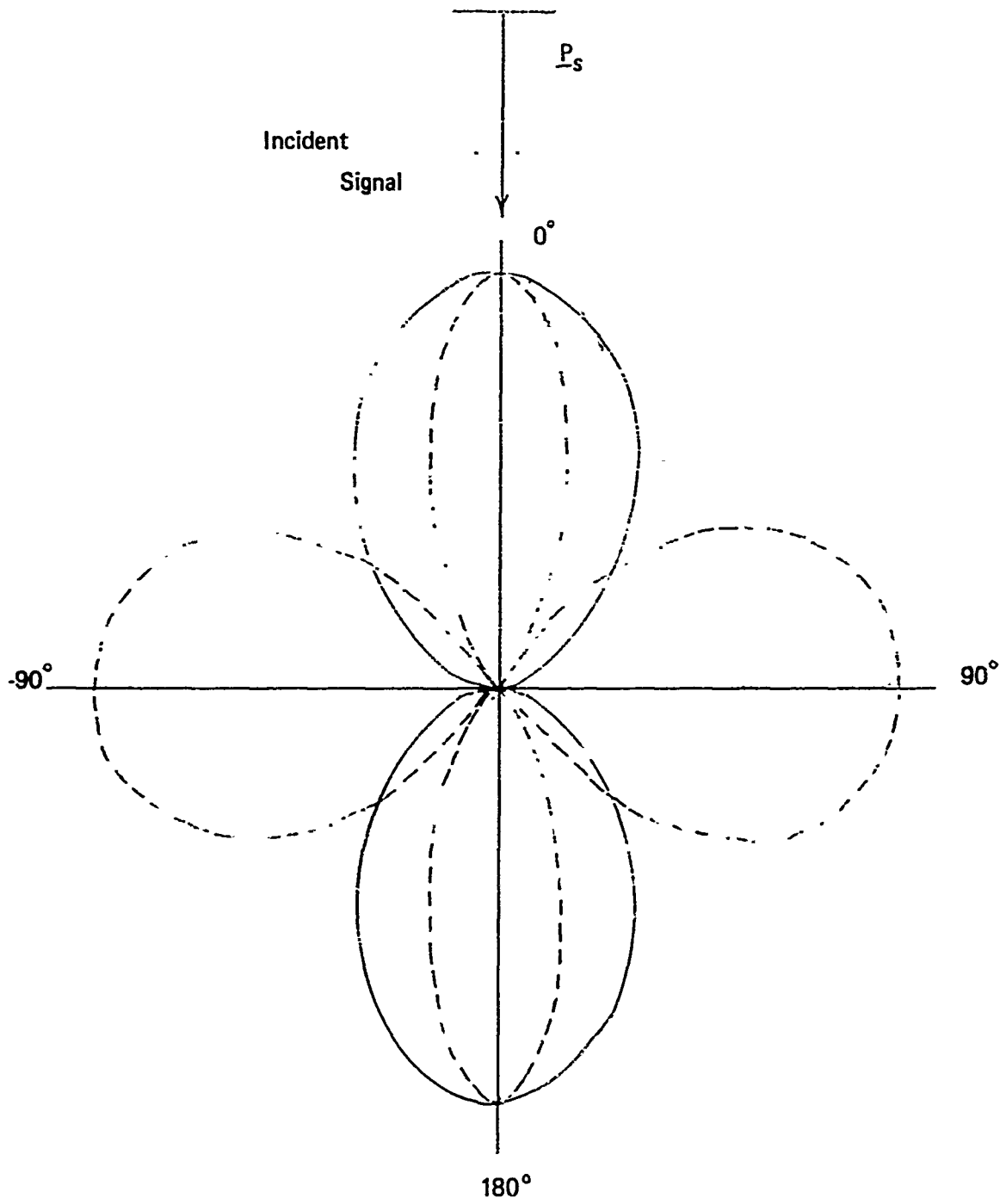


Fig. 5-6. Two-Element Beam Pattern  
(Broadside Signal)

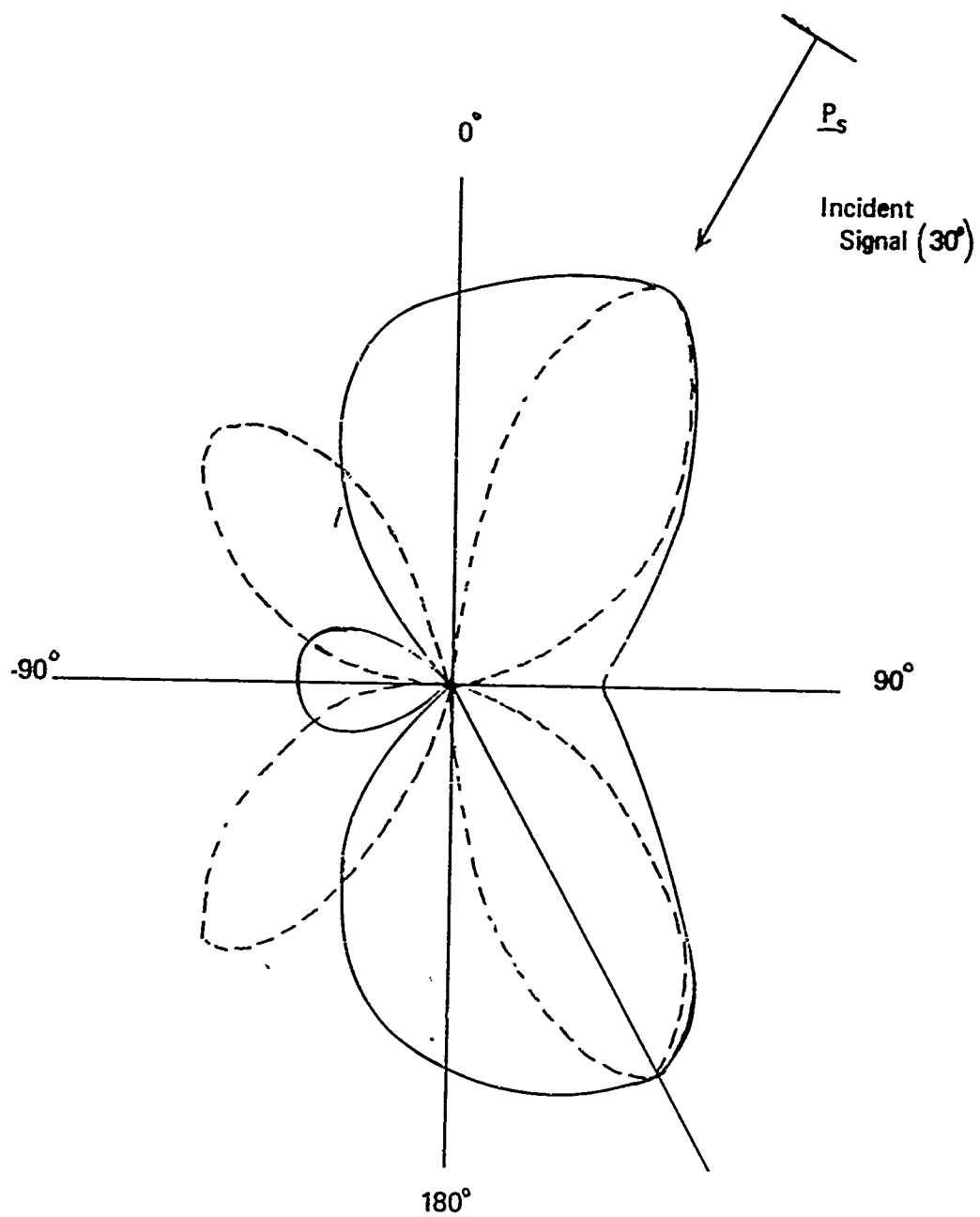


Fig. 5-7. Two-Element Beam Pattern  
(Signal Incident at  $30^\circ$ )

The following case study will investigate the same array receiver in the presence of a multipath signal structure.

5-4. Case III - Two Element Array Correlated Multipath Structure, Coherently Undetectable Case

The preceding case study has shown the system configuration and performance characteristics for a two element array operating in an environment in which there was no multipath. The following case study will investigate the system performance for the same system imbedded in the same noise field environment, but with the random signal now having the multipath structure that was assumed in Case I.

The system configuration is the same as that in figure 5-4, but with  $S_z(\omega)$  now given by equation (5.11) of Case I.

The system performance, a combination of input process SNR given by (5.11) and array gain given by (5.10), is given by equations (5.3) and (5.4) as

$$\delta_o^2 = \int_{-\infty}^{\infty} \left( \frac{\omega_c P_z (A^2 + B^2 + 2AB \cos \omega \Delta)}{\omega_c^2 + \omega^2} \right)^2 \left( 1 - \frac{1}{2} \cos \omega \tau \right)^2 \frac{d\omega}{2\pi} \quad (5.22)$$

where the parameters  $\omega_c$ ,  $P_z$ ,  $\tau$  and  $\Delta$  were defined previously.

Integration of equation (5.22) and numerical evaluation with  $\tau$  fixed and various values of  $A$ ,  $B$ , and  $\Delta$  yield the curves of figure (5.8). In this plot, the normalized effective SNR ( $\delta_o / \text{SNR}$ ) is plotted versus

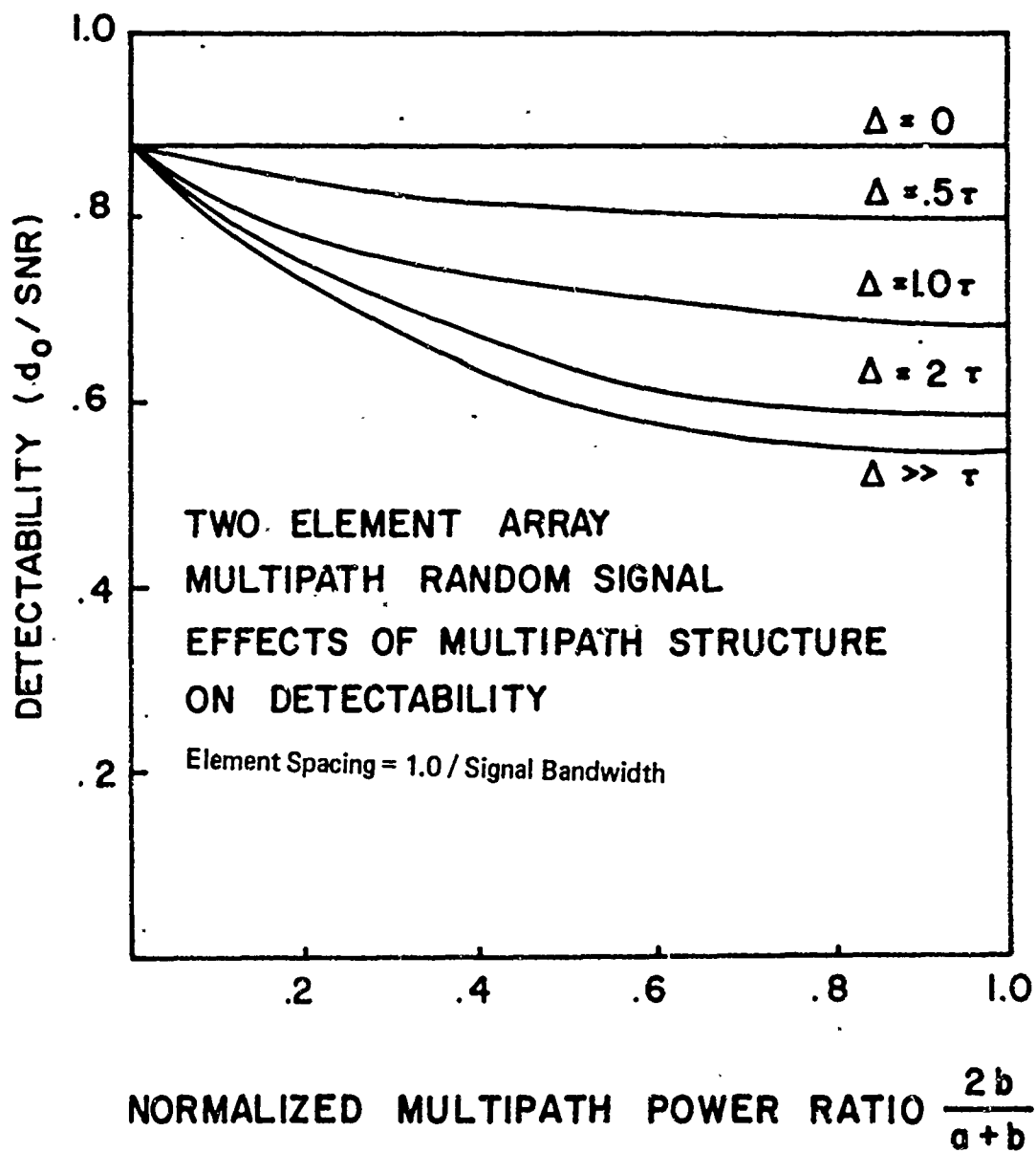


Figure 5-8

the % of power in the second signal for a range of values for  $\Delta$ . The curves show that, for a given element spacing-delay factor  $\tau$ , the system performance degrades as the multipath delay increases, and degrades as a greater percentage of the available signal power is transmitted via the second (later) path. These results show the same trends as for the single element system of Case I. The degradation is again the result of loss of signal energy concentration, resulting in lowered input SNR due to multipath spreading of the random signal. The multipath structure thus causes the same effects in the array detection case as in the single element case.

ROC curves, corresponding to the curves for the index, are plotted in figure 5-9 for fixed multipath power splitting ( $A = 70\%$ ,  $B = 30\%$ ) and varying  $\Delta$  and in 5-10 for fixed  $\Delta$  and varying power splitting ( $.5 \leq A \leq 1.0$ ,  $0 \leq B \leq .5$ ) In both figures limiting "worst" and "best" cases are plotted.

In the above analysis, the effects of changing multipath structure were investigated for fixed element spacing. Since the multipath structure is normally fixed by the physics of the channel, mechanism interacting with the signal, basically uncontrollable, any improvement in system performance due to design must come by variation of the array geometry, steering, or frequency filtering / data processing.

The performance index of (5.22) is plotted in figure 5-11 for fixed multipath structure ( $\Delta = 1.0$ ) and various values of relative element

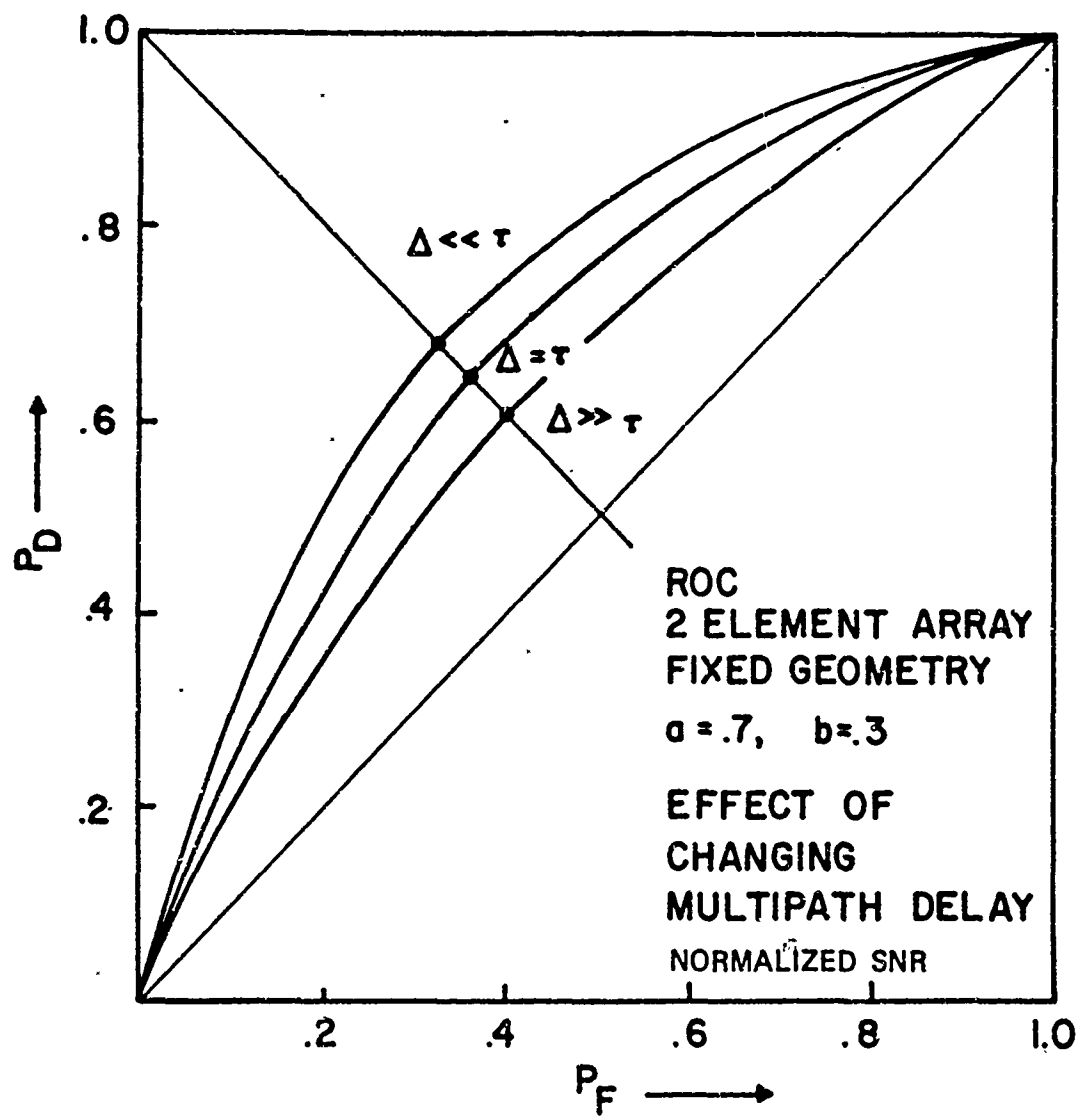


Figure 5-9

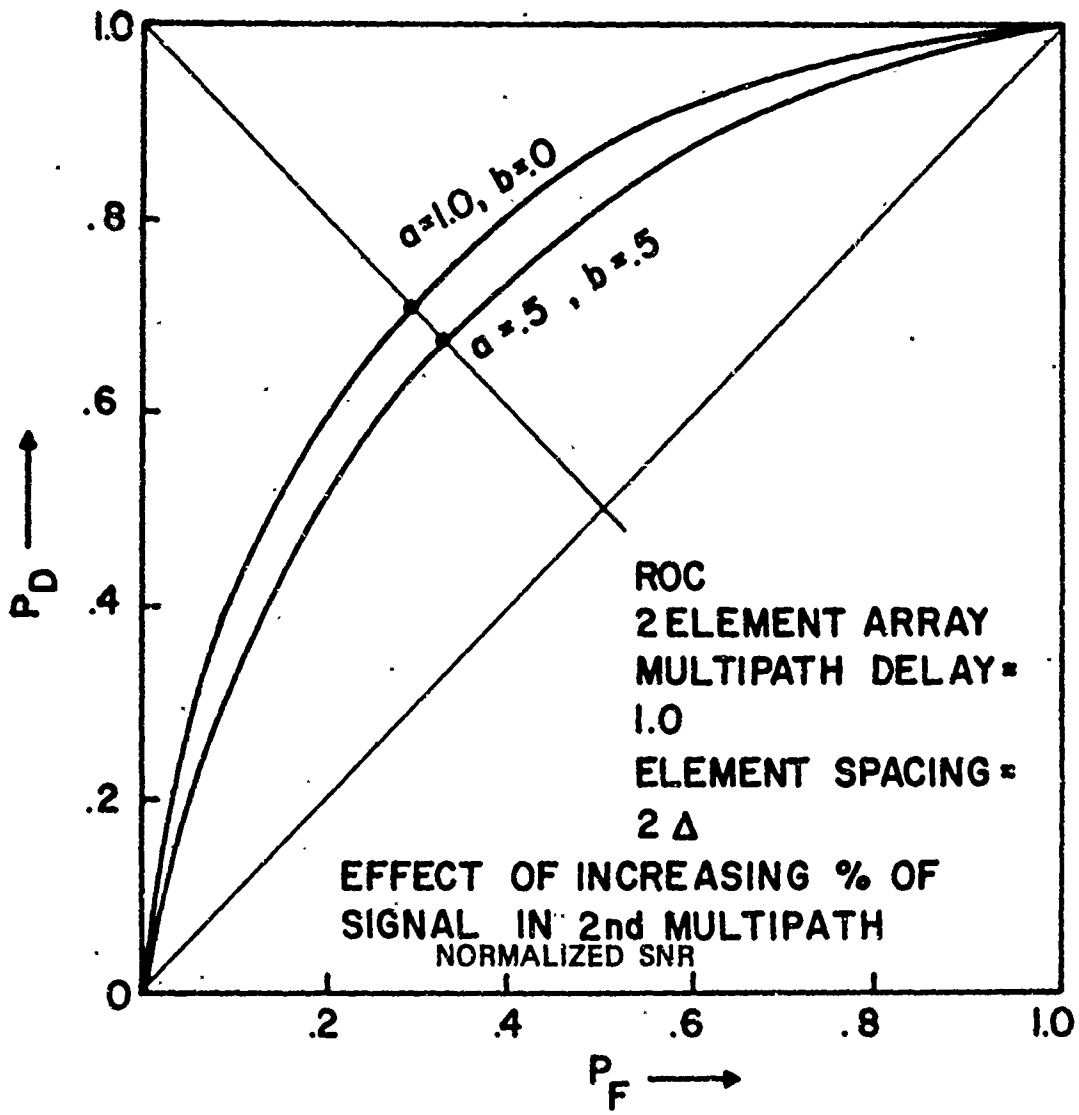
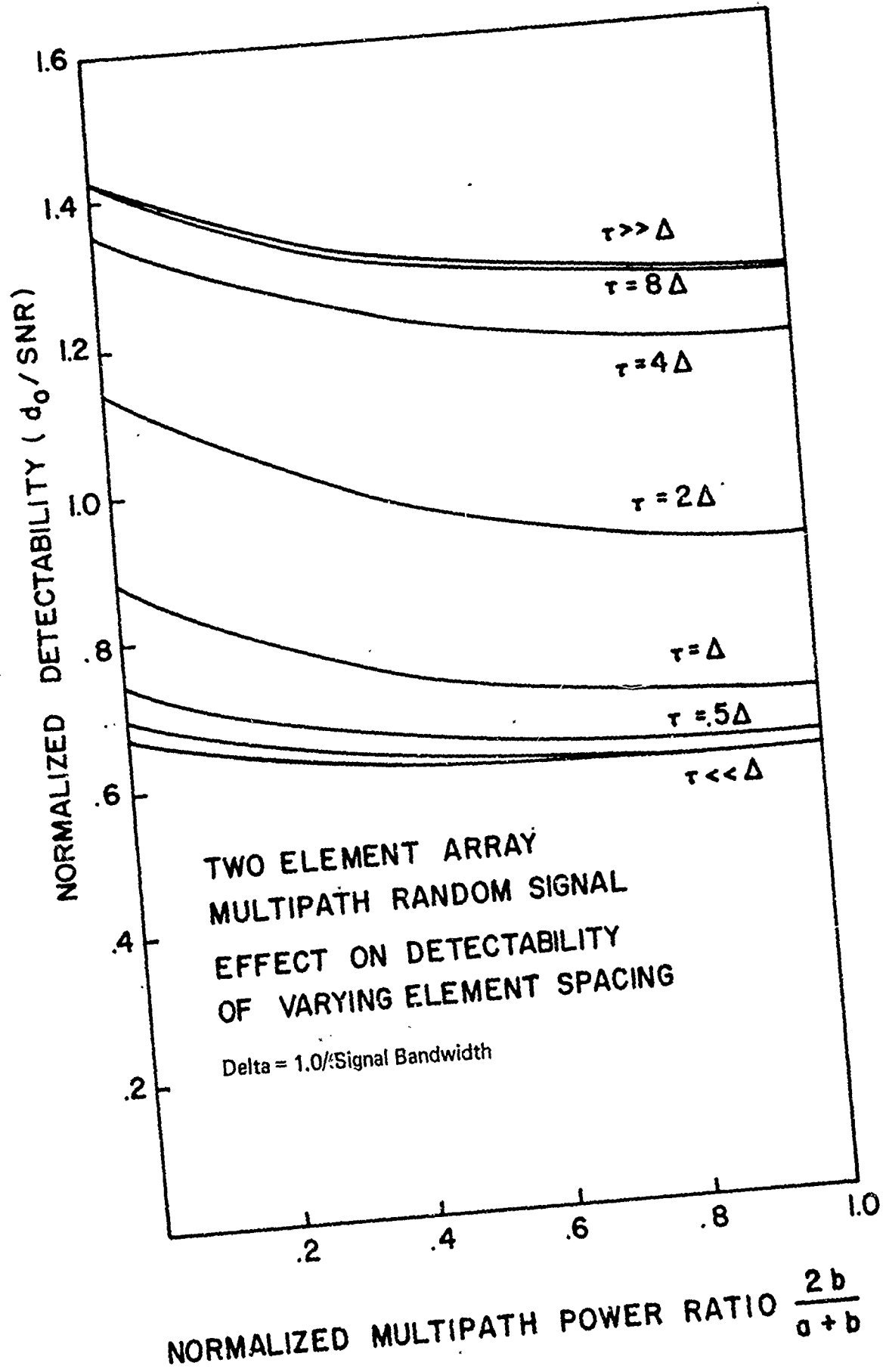


Figure 5-10

Figure 5-11



spacings. These curves show the pronounced effect of element spacing on performance. It can be seen from 5-9 that system performance is enhanced considerably by increasing the separation of the elements.

The interpretation of the variation of performance with element spacing is the same as for Case Study II, and illustrated in Figs. 5-6, 5-7. The increased spacing produces a narrower directional spatial beam pattern with better resolution and the effects of the new combining and frequency filtering stages perform optimal noise and sidelobe rejection, resulting in improved performance. Thus array detectability resolution is increased by separation of the array elements. The ROC curves for a fixed multipath structure are plotted in figure 5-12, showing the effects of array element separation upon system error probabilities. Thus, varying element geometry in the form of separation gives one a method of combating degradation due to multipath.

A comparison of the results of Case Study I and Case Study III are shown in figures 5-13, 5-14, 5-15, 5-16. The figures show a comparison of the performance index of a single element system and a two element array for a range of multipath situations. It will be noted that in each figure, regardless of  $\Delta$ , the curve of the system index  $d$  for the single element lies below the curve for the array index, corresponding to an element spacing of  $\tau=2.0$ . For  $\tau < 2.0$ , the single element performance index is superior to the array system. Since  $\tau$  was plotted relative to the random signal bandwidth in the figures, it is related to  $\omega_c$  by

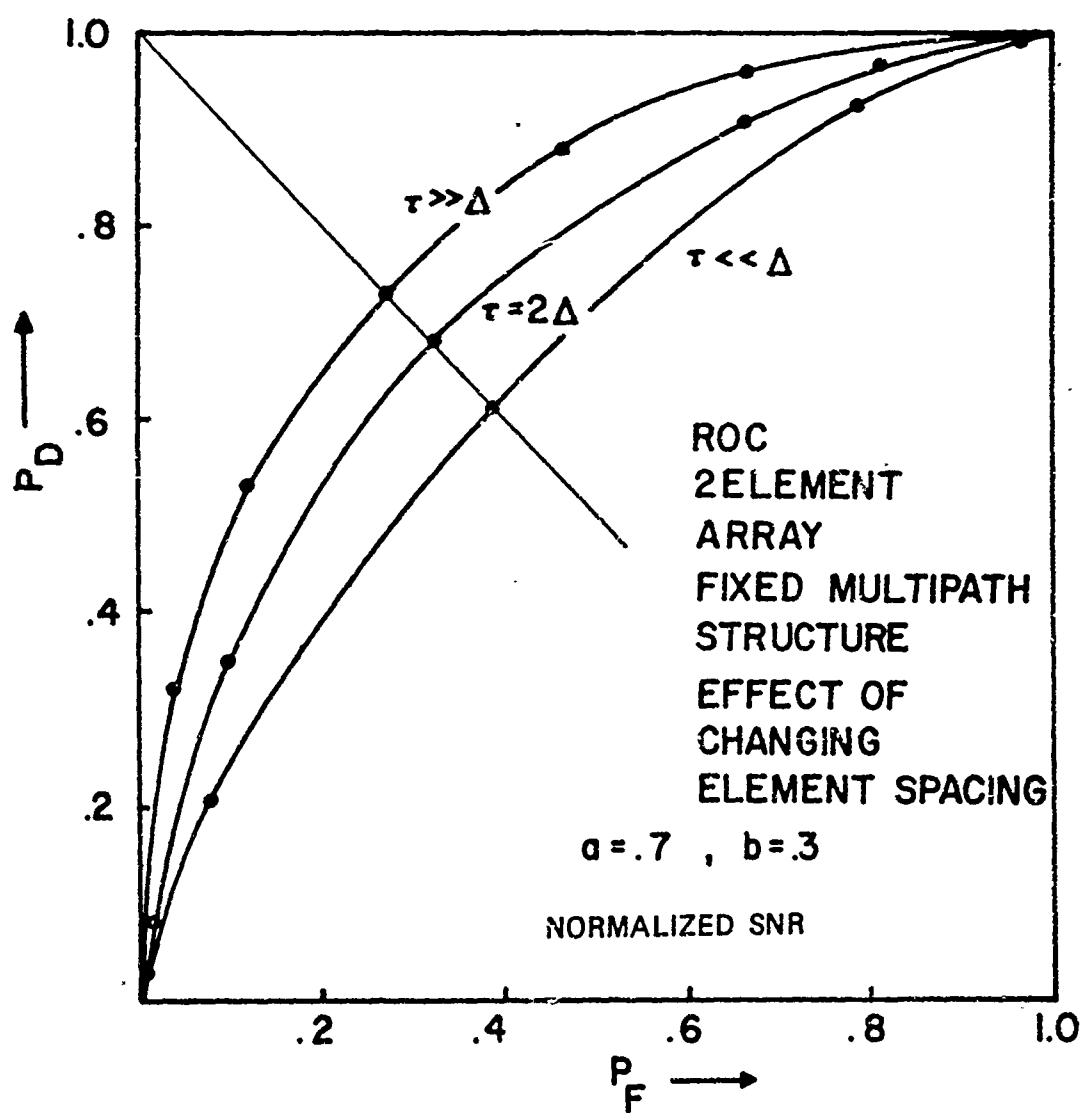


Figure 5-12

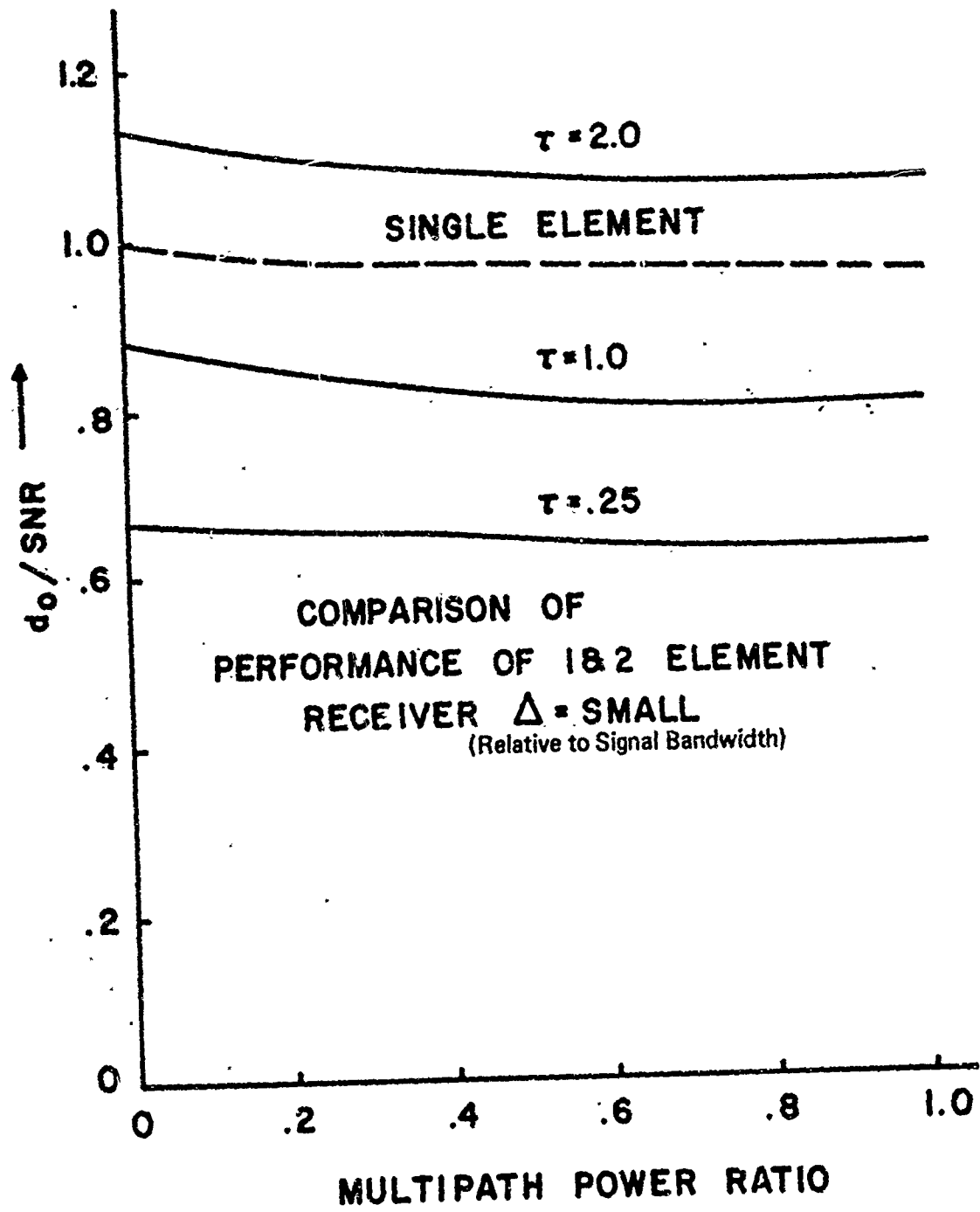


Figure 5-13 .

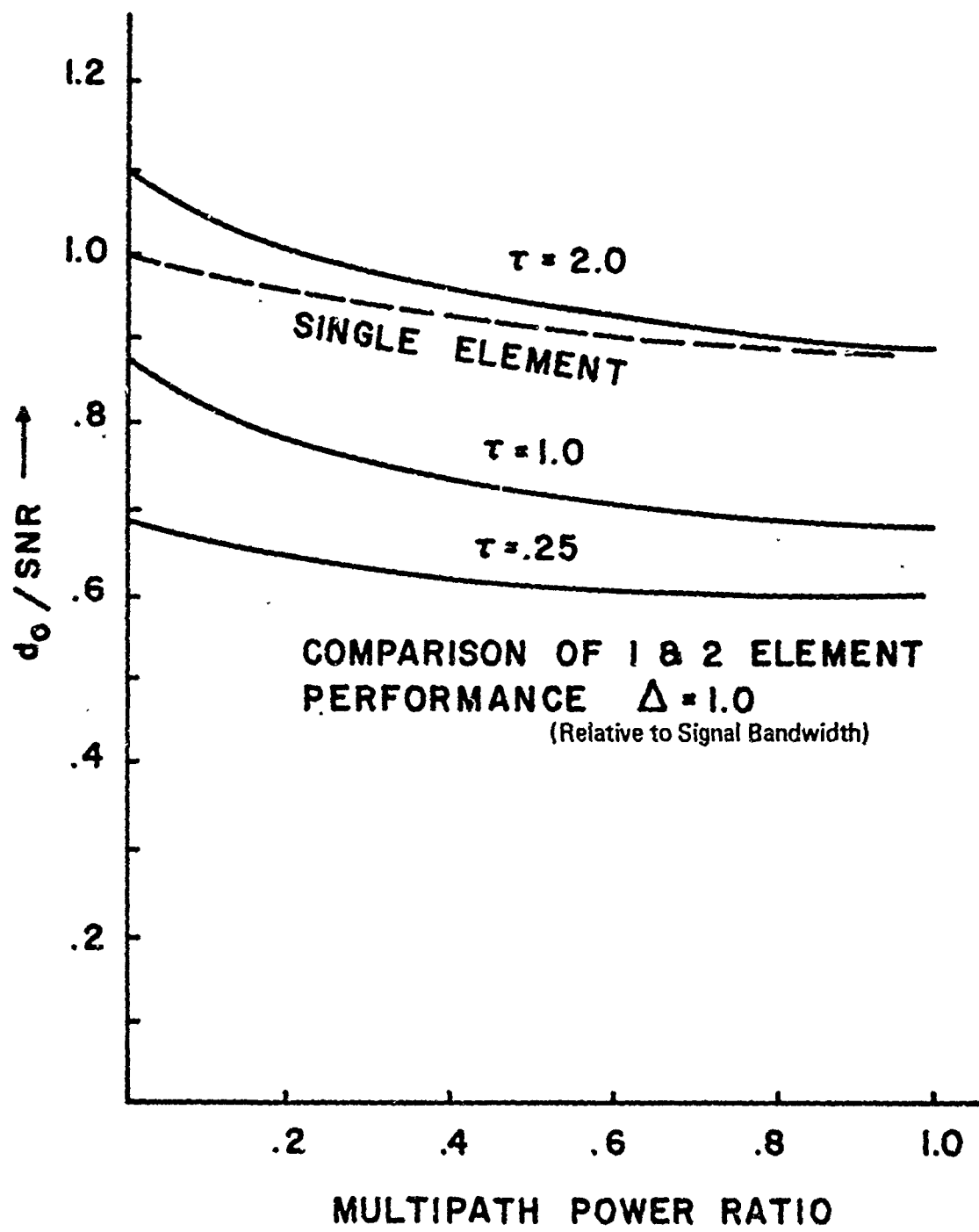


Figure 5-14

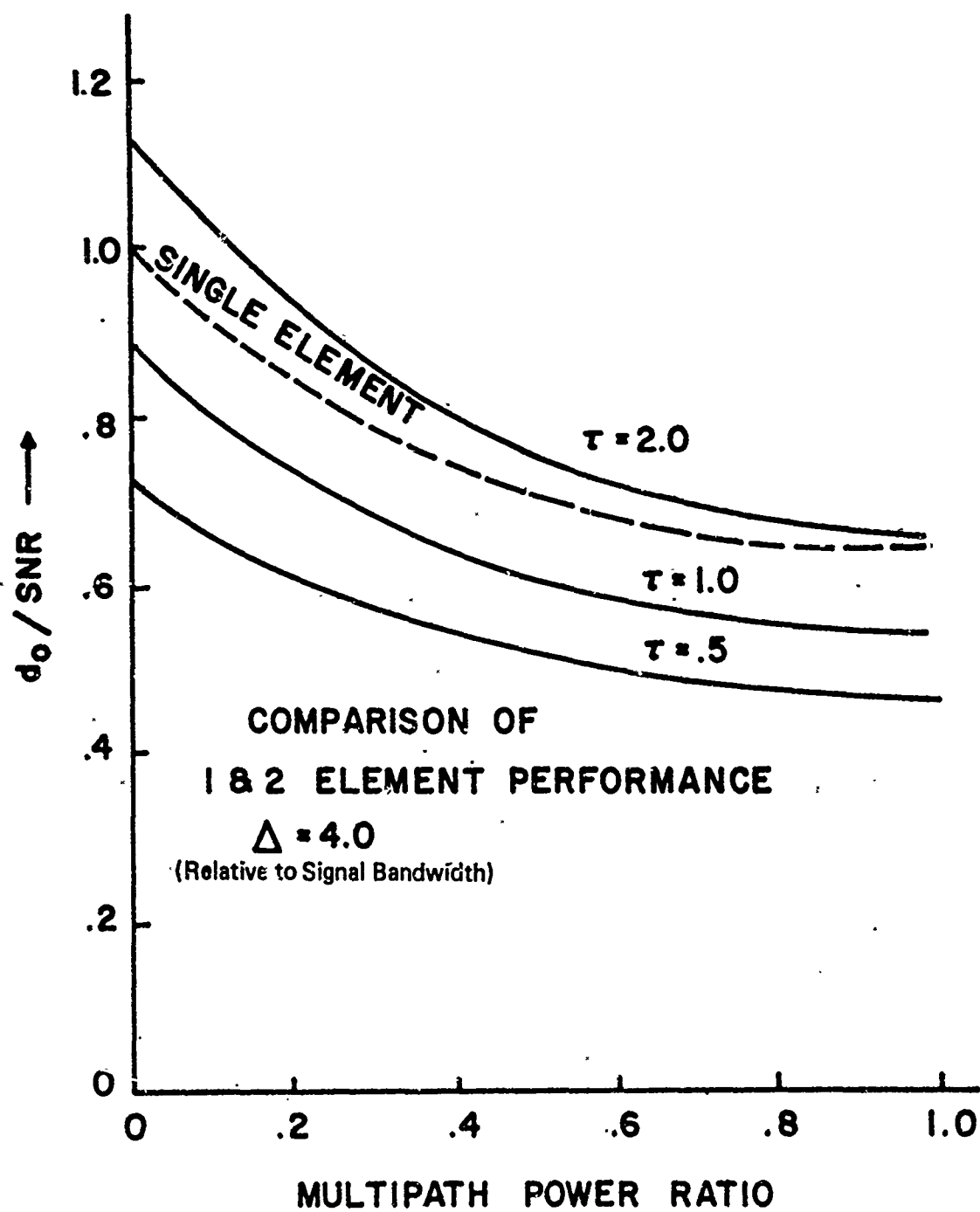


Figure 5-15

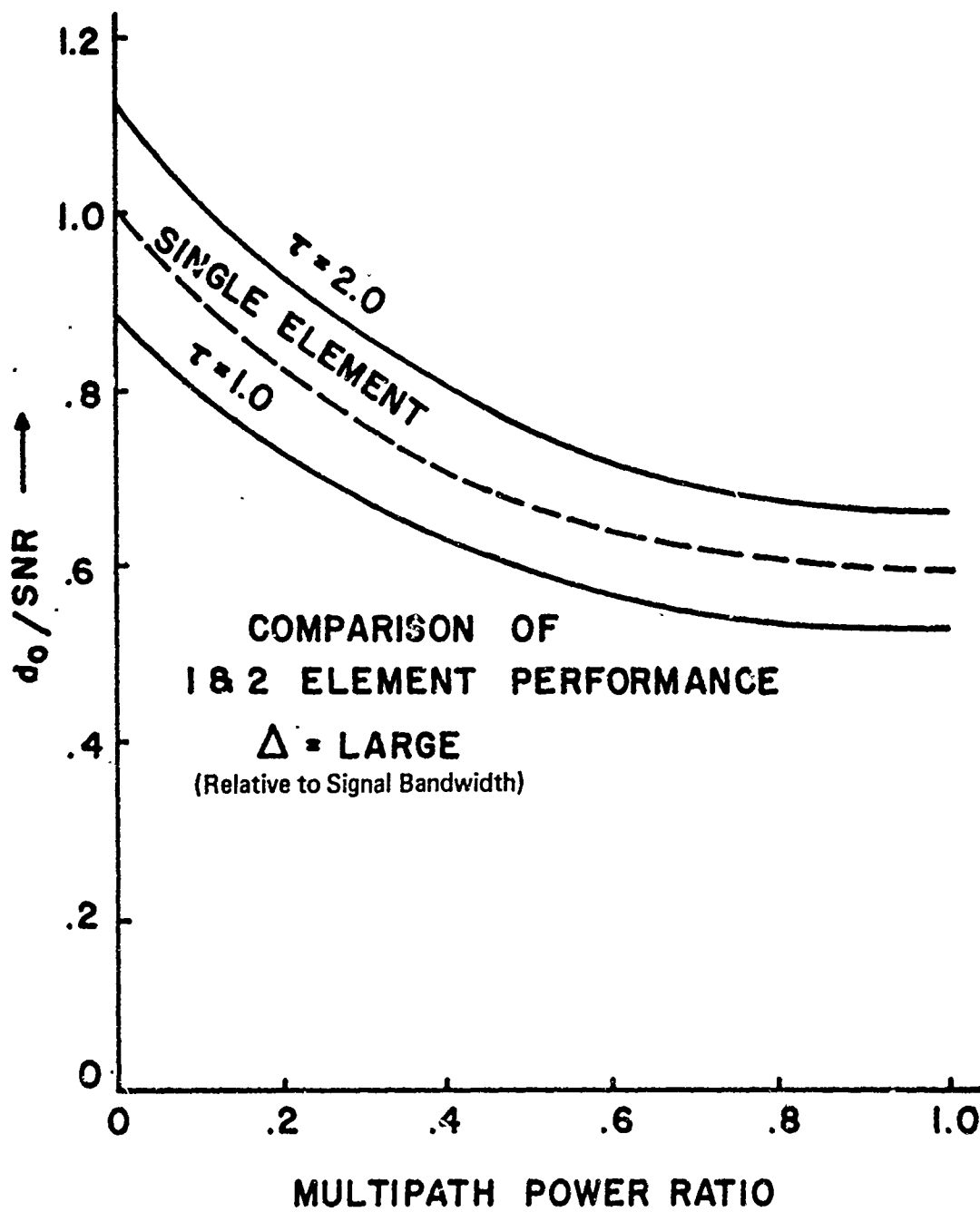


Figure 5-16

$$\tau = \frac{m}{\omega_c}$$

where  $m$  is a positive number dependent upon element spacing and geometry. It follows from examination of the curves of figures 5-13, 5-14, 5-15, 5-16 that the array element spacing must be greater than 2.0 times the reciprocal random signal process bandwidth in order for a two element system to perform more optimally than a single element system. For white noise increasing the spacing beyond  $2.0/\omega_c$  produces even greater improvement in performance, and the array system is clearly preferable. If  $\tau < 2.0$ , the single element receiving system is preferable. Thus, the conclusion is drawn that the key in choosing array geometry (element spacing) for a multipath signal environment is that the element spacing be significantly larger than the reciprocal signal process bandwidth. An improved array system detection performance capability is realized by choosing an element spacing with respect to the power spectrum bandwidth of the incident signal, not with respect to the multipath structure in this case. The array geometry should be chosen to give "best" performance possible (as widely spaced elements as technically feasible) under the assumption that there is no multipath structure in the random signal. If  $\tau > 2.0/\omega_c$ , this insures that the array will give superior performance over the single element. If a multipath structure does actually exist, the performance will degrade simultaneously compatible amounts in both systems, as is shown by comparing figures

5-13 through 5-16 If the multipath structure is fixed, the major method available to the designer to improve a system's performance is to increase the element spacing; once the maximum spacing (dictated by practical size and space requirements) is reached, and if  $\tau > 2.0/\omega_c$ , performance is optimal. This dependence results from the separation of array gain function (noise field and steering effects) and the signal-to-noise-ratio (random signal field, multipath effects) in the performance index. The use of multiple element detection systems with proper element spacing can be used to overcome degradation in a single element system caused by the multipath. The above assumes that desired spacing can be achieved such that the receiving elements are located in a manner which renders cross-link noise correlation zero.

In general, the preceding case study has shown that

1. system performance degrades as the multipath delay increases
2. system performance degrades as more signal energy is transmitted via later paths
3. system performance improves as the element separation is increased
4. two element system performance is optimal over a single element system for array spacing greater than 2.0 times the reciprocal bandwidth of the random signal in any given multipath environment, assuming approximately

a single arrival direction.

The above case study establishes the utility of array/diversity receiving systems and illustrates a method of evaluating attainable performance capability over single receiving element systems.

5-5. Case IV - Multi-Element Array, Optimum Geometry, No Multipath

The above studies have shown that the "best" performance for a multi-element array is realized for an array with widely spaced elements imbedded in a channel with no multipath. In such cases, the performance characteristics are optimum. ROC curves for a single element, a two element, and a three element receiver in such an optimum environment are shown in figure 5-17. In this plot, the performance of multi-element detection systems is illustrated. Curves for systems  $N > 3$  lie above the  $N = 3$  curve and have superior performance characteristics. Thus detection capability can be enhanced by properly employing optimized multi-element arrays. In general, properly designed space-time multi-element array detection systems offer more flexibility and superior system performance characteristics than do systems employing a single element.

5-6. Summary

The series of case studies has shown the effects upon system performance (error probabilities and detectability) in terms of

- 1) multipath structure in the incident random signal (multipath delay and

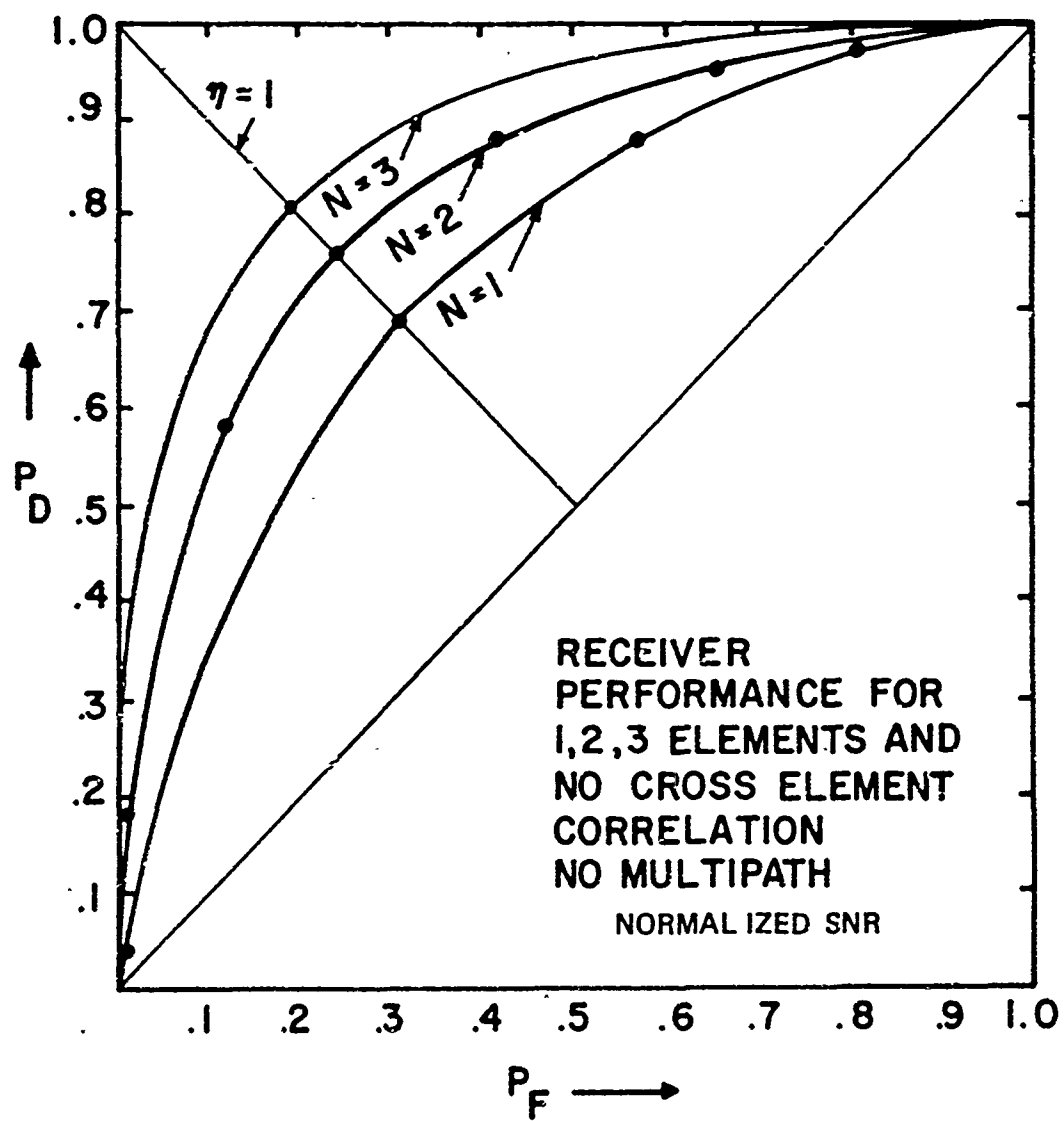


Figure 5-17

multipath power division), 2) array geometry and steering (element spacing), and 3) space-time (spatio-temporal) correlation properties of the incident random processes. In general, the following conclusions can be established:

1. Pronounced multipath structure in the random signal degrades system performance due to spreading of the signal energy over time. Increasing delay and power split degrade performance, with the delay factor being the major factor in degrading performance.
2. Multi-element systems suffer comparable degradation in performance resulting from multipath, as do single element systems.
3. Multi-element systems offer better performance characteristics than single element systems, if the spacing of the array elements is greater than  $m$  times the reciprocal bandwidth of the incident random signal; where  $m$  is a constant dependent upon the number of elements, the signal and noise fields, and the array geometry. For  $N=2$ , an interferometer,  $m \approx 2.0$ .
4. The maximum performance gain possible for the cases considered is realized for large element spacing.
5. The array system requirements and performance characteristics are highly dependent upon the spatial structure

of the array and the space-time structure of the incident signal and interference fields.

6. The array space-time analysis technique is an extremely powerful tool for analysis, design, implementation, and evaluation of modern detection systems.

## CHAPTER VI

### CONCLUDING REMARKS AND FUTURE RESEARCH

It has been the purpose of this research effort to obtain definitive solutions to the problems associated with the analysis and design of optimal space(array)diversity receiving systems. In particular, it is of considerable technological interest to establish the optimum system requirements and system configurations, and to ascertain their related performance characteristics for a wide range of physical information channel, cross-section and noise field environments. The results and conclusions obtained in this effort offer considerable design improvement capability in the areas of sonar/radar/communications/seismology, as well as offering a unified, more concise formulation for many general reception/detection/estimation problems.

This effort, along with other studies in spatio-temporal reception (Refs. 1, 2, 14, 20-24, 46) has shown that the dichotomy of the detection problem into two separate areas (antenna and sensor design, and statistical communication theory) can result in design and implementation of receiver systems that are not truly optimum, in the sense of maximum exploitation of the available information and physics of the environment. Space-time considerations attempt to combine the spatial properties and the temporal properties of the incident processes physics, the array, its geometry, and the associated data processor in order to obtain

systems that are optimum in both their space and their time data processing characteristics. It has been shown that such systems, when properly designed, offer performance improvement over sub-optimum systems implemented with limited "classically optimal" procedures. This improved performance is not obtained without cost, however, since the analysis and design of space-time systems is considerably more difficult than conventional methods. Thus, performance enhancement is possible by the use of spatio-temporal techniques, enhancement that is paid for by larger, more complex, yet quite physically tractable, systems.

Finally, the effort has shown that in the final analysis, in design and implementation of receiving systems, the engineer must deal with the real, basic physics of wave mechanics and receiving element-wave front interaction. The mathematical elegance, abstractness, and complexity that arises in the analysis, is only of value if it reflects and models the actual physical mechanisms that exist in the physical environment of the systems. The goal in engineering, and in particular, in space-time reception, is to express the system requirements and resulting performance in terms of the fundamental variables of physics (space, time and energy). Solutions not in these terms, or not capable of being reduced to them, are of little practical engineering value. It has been the purpose of this research to express the results in terms of these variables.

This research effort has quantitatively established the optimum system requirements and configurations, and quantitatively established the effects upon system performance of

1. multipath structure in the random signal, both variations in the path delay and power division between the various paths.
2. the effects of array element separation (array geometry) relative to the structure of the incident processes
3. the effects of certain spatio-temporal correlation properties of the incident processes.

In particular, it was found that

1. increasing multipath delay degrades performance, as does spreading of the available signal power over a number of transmission paths
2. in array detection, the key relationship is the signal bandwidth to element spacing. If the spacing is such that it is approximately 2.0 times the reciprocal bandwidth of the random signal, the array will perform in a superior manner when compared to a single element system. Decreasing the spacing below this value yields the single receiving element system preferable.
3. the optimum system configuration in a two element array is such that the elements are as widely separated as possible.

Finally, some criticism of the preceding analysis is necessary; these criticisms give rise to future necessary studies and further research efforts.

The most obvious need is for the analysis to be extended to multiple element ( $N > 2$ ) arrays. The analysis methods presented here are valid for these larger arrays. This study ( $N = 2$ ) gives insight into the effects and shows the general trends of the effects of element spacing and multipath upon system performance. Analysis for ( $N > 2$ ) will give more definitive answers as to the effect of element spacing and geometry in multi-element systems.

Additional study is needed for space-time random fields other than those considered in the case studies. In particular, the effects of the magnitude of cross link correlation of the noise and signal fields need to be established. The analysis presented above considered only white noise and Markovian signals; other distributed noise field spectra should be investigated.

The multipath arrival angle in the cases was assumed essentially the same for all paths. In practice, the angles are usually different; this analysis needs to be investigated further. A recent effort by Schweppe<sup>46</sup> has initiated a study of this area.

The signals were considered purely random. Middleton<sup>18</sup> has shown that a strong specular component is present quite often in the cases of random fading, scattering, and reverberation of deterministic

signals. This result should be incorporated into the system design equations.

Finally, the analysis was carried out by assuming that the coupling was memoryless. The analysis should include the specific effects of the interaction of the receiving elements and the space-time wave equations. Such multivariable analysis<sup>14, 18</sup> would strengthen the arguments for consideration of the unified space-time reception problem.

In effect, this research is only the beginning of a much broader, more general research effort that has been critically needed in studying the reception problem. There is a definite need to reorganize and unify the disciplines of statistical communication theory and antenna array design theory in order to achieve a unified approach to the solution of the reception problem. This research effort has investigated a small area of the total problem. It has shown that space-time analysis is definitely valuable in system design and has given definitive, quantitative answers to the case study problems of optimum array detection of noisy random multipath signals. It has established the effects of multipath (delay and power division), of element geometry (spacing), and of spatio-temporal correlation properties of the incident random fields on performance.

The over-all result of this research effort is the establishing of general synthesis guidelines that enable one to attain, design, implement, analyze, and enhance performance of optimum space-time detection/estimation/classification/ and discrimination systems.

## REFERENCES

1. R. F. White, "Space Diversity on Line-of-Sight Microwave Systems," *IEEE Transactions on Communications Technology*, Vol. COM-16, No. 1, February, 1968, pp. 119-132.
2. B. Widrow, P. E. Mantey, L. J. Griffiths, and B. B. Goode, "Adaptive Antenna Systems," *Proc. IEEE*, Vol. 55, No. 12, December, 1967, pp. 2143-2158.
3. F. P. Cusanno, "Tropospheric Scatter Propagation and Equipment Performance Results Obtained on a System in Korea," *Trans. IEEE*, Vol. COM-15, No. 5, October, 1967, pp. 694-699.
4. J. D. Kraus, Antennas, McGraw-Hill, New York, 1950.
5. C. H. Papas, Theory of Electromagnetic Wave Propagation, McGraw-Hill, New York, 1965.
6. \_\_\_\_\_, Microwave Scanning Antennas, R. C. Hansen, Ed., Academic Press, New York, 1966.
7. R. Price, "Optimum Detection of Random Signals in Noise, with Applications to Scatter Multipath Communication," *Trans. PGIT-IRE*, Vol. IT-2, No. 4, December, 1956, pff. 125.
8. R. Price, "Output Signal-to-Noise Ratio as a Criterion in Spread Channel Signalling," M. I. T. Lincoln Lab. R. R. 388.
9. R. Price, "Optimum Detection of Random Signals Perturbed by Scatter and Noise," *IRE Trans.*, PGIT-4, September, 1954, pp. 163-170.
10. T. Kailath, "Correlation Detection of Signals Perturbed by a Random Channel," *IRE Trans.*, Vol. IT-6, No. 3, June, 1960, pp. 361-366.
11. W. B. Davenport, Jr., and W. L. Root, Random Signals and Noise, McGraw-Hill, New York, 1958.

12. L. A. Wainstein and V. D. Zubakov, Extraction of Signals from Noise, Prentice-Hall, London, 1962.
13. C. W. Helstrom, Statistical Theory of Signal Detection, Pergamon Press, 1960.
14. H. L. Van Trees, Detection Estimation and Modulation Theory, I, II, Wiley, New York; Vol. I, 1968, Vol. II, to be published 1968-69.
15. F. Bryn, "Optimum Signal Processing of Three-Dimensional Arrays Operating on Gaussian Signals and Noise," J. Acoust. Soc. Amer., Vol. 34, March, 1962, pp. 289-297.
16. E. J. Kelly, "A Comparison of Seismic Array Processing Schemes," Tech. Note 1965-21, M. I. T., Lincoln Lab., June, 1965.
17. P. Green, E. Kelly, and M. Levin, "A Comparison of Seismic Array Processing Methods," Geophys. J. Royal Astronomical Society (6B), Vol. 11, pp. 67-84, 1966.
18. D. Middleton, "A Statistical Theory of Reverberation and Similar First-Order Scattered Fields, I, II, IEEE Trans., Vol. IT-13, No. 3, July, 1967, pp. 372-413.
19. E. J. Kelly and M. J. Levin, "Signal Parameter Estimation for Seismometer Arrays," Lincoln Laboratory Tech. Report 339, January, 1964.
20. D. G. Childers, "Generalized Spatio-temporal Correlation Functions for Antennas," Trans. IEEE, Vol. IT-13, No. 1, January, 1967, pp. 121-122.
21. N. T. Gaarder, "Maximal-Ratio Diversity Combiners," Trans. IEEE, Vol. Com-16, No. 6, December, 1967, pp. 790-796.
22. J. H. Derryberry and W. D. Gregg, "On the Performance Characteristics of Maximum Likelihood Diversity Array Receivers," Proc. of Southwestern IEEE 1968, April, 1968, pp. 21B.
23. D. K. Cheng and F. I. Iseng, "Optimum Spatial Processing in a Noisy Environment for Arbitrary Antenna Arrays Subject to Random Errors," IEEE Trans. Antennas and Propagation, Vol. AP-16, No. 2, March, 1968, pp. 164-171.

24. N. T. Gaarder, "Design of Point Detector Arrays, I,"  
Trans. IEEE, Vol. IT-13, No. 1, January, 1967,  
pp. 42-50.
25. R. B. Blackman, Data Smoothing and Prediction, Addison  
Wesley, New York, 1965.
26. D. Middleton, Introduction to Statistical Communication Theory,  
McGraw-Hill, 1960.
27. T. W. Anderson, An Introduction to Multivariate Statistical  
Analysis, Wiley and Sons, New York, 1958.
28. M. Schwartz, W. R. Bennet, and S. Stein, Communication  
Systems and Techniques, McGraw-Hill, New York, 1966.
29. H. Reed and C. Russell, Ultra High Frequency Propagation,  
Boston Tech. Publishers, Cambridge, 1966.
30. M. Nesenbergs, "Error Probability for Multipath Fading,"  
Trans. IEEE, Vol. Com-15, No. 6, December 1967,  
pp. 797-804.
31. R. T. Aiken, "Communication Over the Discrete-Path Fading  
Channel," Trans. IEEE, Vol. IT-13, No. 2, April, 1967,  
pp. 346-348.
32. W. Vanderhulk, "Optimum Processing for Acoustic Arrays,"  
J. of British Inst. of Radio Engr., Vol. 26, No. 4,  
October, 1963, pp. 285-293.
33. E. J. Kelly and W. L. Root, "A Representation of Vector-  
Valued Random Processes," J. Math. and Phys.,  
Vol. 39, No. 3, October, 1960, pp. 211-216.
34. R. Courant and D. Hilbert, Methods of Mathematical Physics,  
Interscience Publishers, New York, 1960.
35. F. B. Hildebrand, Methods of Applied Mathematics, Prentice-  
Hall, Englewood Cliffs, New Jersey, 1952.
36. R. Price and P. E. Green, Jr., "Signal Processing in Radar  
Astronomy - Communication via Fluctuating Multipath  
Media," M. I. T., Lincoln Lab. TR-234, October, 1960.

37. R. E. Kalman, "A New Approach to Linear Filtering and Prediction Problems," J. Basic Engr., ASME Trans., 82D, 1960, pp. 35-45.
38. A. Papoulis, Probability, Random Variables, and Stochastic Processes, McGraw-Hill, New York, 1965.
39. K. S. Miller, Multidimensional Gaussian Distributions, Wiley and Sons, New York, 1964.
40. E. D. Nering, Linear Algebra and Matrix Theory, Wiley and Sons, New York, 1963.
41. M. Masonson, "On the Gaussian Sum of Gaussian Variates, the Non-Gaussian Sum of Gaussian Variates, and the Gaussian Sum of Non-Gaussian Variates," Proc. IEEE, Vol. 55, No. 9, September, 1967, pp. 1661-1663.
42. D. Middleton, "Estimating the Noise Power of an Otherwise Known Noise Process," IDA, July 1963
43. B. B. Goode, "Synthesis of a Nonlinear Bayes Detector for Gaussian Signal and Noise Fields Using Wiener Filters," Trans. IEEE, Vol. IT-13, No. 1, January, 1967, pp. 116-118.
44. J. K. Butler, "Antenna Array Excitation for Maximum Gain," Proc. IEEE, Vol. 56, No. 1, January, 1968, pp. 85-89.
45. J. Kraus, Radio Astronomy, McGraw-Hill, New York, 1966.
46. F. C. Schweppe, "Sensor-Array Data Processing for Multiple-Signal Sources," IEEE Trans., Vol. IT-14, No. 2, March, 1968, pp. 294-305.

UNCLASSIFIED  
Security Classification

DOCUMENT CONTROL DATA - R&D		
<i>(Security classification of title, body of abstract and indexing annotation must be entered when the overall report is classified)</i>		
1. ORIGINATING ACTIVITY (Corporate author) The University of Texas at Austin Electronics Research Center Austin, Texas 78712		2a. REPORT SECURITY CLASSIFICATION <b>UNCLASSIFIED</b>
		2b. GROUP
3. REPORT TITLE  ON OPTIMUM SPACE DIVERSITY RECEPTION OF CORRELATED MULTIPATH		
4. DESCRIPTIVE NOTES (Type of report and inclusive dates) Scientific Interim		
5. AUTHOR(S) (Last name, first name, initial)  Jim H. Derryberry                  William D. Gregg		
6. REPORT DATE 14 June 1968	7a. TOTAL NO. OF PAGES 113	7b. NO. OF REFS 46
8a. CONTRACT OR GRANT NO. AF-AFOSR-67-766A	9a. ORIGINATOR'S REPORT NUMBER(S)  JSEP, Technical Report No. 50	
b. PROJECT NO. 4751		
c. 6144501F	9b. OTHER REPORT NO(S) (Any other numbers that may be assigned this report) OSR 68-1657	
d. 681305		
10. AVAILABILITY/LIMITATION NOTICES 1. This document has been approved for public release and sale; its distribution is unlimited.		
11. SUPPLEMENTARY NOTES  TECH, OTHER	12. SPONSORING MILITARY ACTIVITY JSEP through AF Office of Scientific Research (SREE) 1400 Wilson Boulevard Arlington, Virginia 22209	
13. ABSTRACT  This research effort investigates system requirements, configurations, and associated performance characteristics of maximum-likelihood space-diversity receiving systems. From the maximum-likelihood principle, and the multidimensional Karhunen-Loeve expansion, the continuous decision equations for space-time detection of noisy, random multipath signals are developed. Interpretation of these equations yields the optimum space-time receiving system configuration requirements.  The performance characteristics of the resultant systems are then analyzed to determine the effects of channel multipath structure (multipath delay and power division among the paths), space-time correlation properties of the incident processes, and the specific temporal correlation introduced by the array geometry. It is shown by a series of case studies, that for both the single element coupling as well as array multiple element coupling, that increasing the multipath delay factor results in decreased system performance capability for fixed power of the signal and noise processes. Similarly, the performance capacity is degraded as the available signal power tends to distribute more equally over the multiple transmission paths. These effects are attributed to the loss of effective signal energy concentration, resulting in a lower effective detectability signal-to-noise ratio. An investigation of these effects upon system performance, due to array geometry (receiving element spacing) shows that performance is enhanced by increasing the separation distance of the elements for a given multipath situation. This phenomena is the result of a more compatible array beam pattern that comes about from increased spacing. In effect, with increased spacing, the main lobe of the pattern is narrowed, while the side lobes are optimally suppressed by the optimal cross-coupling of elements. Finally the analysis illustrates how optimum space-time receiving systems capability results from a joint consideration of the coupling and temporal processing, rather than a dichotomization of the problem into a spatial (antenna) problem and a (temporal) data processing problem. As such, the analysis yields a more concise, broader, interpretation of system design requirements and associated performance characteristics.		

**UNCLASSIFIED**  
Security Classification

14. KEY WORDS	LINK A		LINK B		LINK C	
	ROLE	WT	ROLE	WT	ROLE	WT
MULTIPLE ELEMENT FIELD COUPLING ARRAY RECEPTION MAXIMUM LIKELIHOOD DETECTION OPTIMAL RECEPTION OF CORRELATED MULTIPATH OPTIMAL SPACE DIVERSITY						

**INSTRUCTIONS**

**1. ORIGINATING ACTIVITY:** Enter the name and address of the contractor, subcontractor, grantee, Department of Defense activity or other organization (*corporate author*) issuing the report.

**2a. REPORT SECURITY CLASSIFICATION:** Enter the overall security classification of the report. Indicate whether "Restricted Data" is included. Marking is to be in accordance with appropriate security regulations.

**2b. GROUP:** Automatic downgrading is specified in DoD Directive 5200.10 and Armed Forces Industrial Manual. Enter the group number. Also, when applicable, show that optional markings have been used for Group 3 and Group 4 as authorized.

**3. REPORT TITLE:** Enter the complete report title in all capital letters. Titles in all cases should be unclassified. If a meaningful title cannot be selected without classification, show title classification in all capitals in parenthesis immediately following the title.

**4. DESCRIPTIVE NOTES:** If appropriate, enter the type of report, e.g., interim, progress, summary, annual, or final. Give the inclusive dates when a specific reporting period is covered.

**5. AUTHOR(S):** Enter the name(s) of author(s) as shown on or in the report. Enter last name, first name, middle initial. If military, show rank and branch of service. The name of the principal author is an absolute minimum requirement.

**6. REPORT DATE:** Enter the date of the report as day, month, year, or month, year. If more than one date appears on the report, use date of publication.

**7a. TOTAL NUMBER OF PAGES:** The total page count should follow normal pagination procedures, i.e., enter the number of pages containing information.

**7b. NUMBER OF REFERENCES:** Enter the total number of references cited in the report.

**8a. CONTRACT OR GRANT NUMBER:** If appropriate, enter the applicable number of the contract or grant under which the report was written.

**8b, 8c, & 8d. PROJECT NUMBER:** Enter the appropriate military department identification, such as project number, subproject number, system numbers, task number, etc.

**9a. ORIGINATOR'S REPORT NUMBER(S):** Enter the official report number by which the document will be identified and controlled by the originating activity. This number must be unique to this report.

**9b. OTHER REPORT NUMBER(S):** If the report has been assigned any other report numbers (*either by the originator or by the sponsor*), also enter this number(s).

**10. AVAILABILITY/LIMITATION NOTICES:** Enter any limitations on further dissemination of the report, other than those

imposed by security classification, using standard statements such as:

- (1) "Qualified requesters may obtain copies of this report from DDC."
- (2) "Foreign announcement and dissemination of this report by DDC is not authorized."
- (3) "U. S. Government agencies may obtain copies of this report directly from DDC. Other qualified DDC users shall request through \_\_\_\_\_."
- (4) "U. S. military agencies may obtain copies of this report directly from DDC. Other qualified users shall request through \_\_\_\_\_."
- (5) "All distribution of this report is controlled. Qualified DDC users shall request through \_\_\_\_\_."

If the report has been furnished to the Office of Technical Services, Department of Commerce, for sale to the public, indicate this fact and enter the price, if known.

**11. SUPPLEMENTARY NOTES:** Use for additional explanatory notes.

**12. SPONSORING MILITARY ACTIVITY:** Enter the name of the departmental project office or laboratory sponsoring (*paying for*) the research and development. Include address.

**13. ABSTRACT:** Enter an abstract giving a brief and factual summary of the document indicative of the report, even though it may also appear elsewhere in the body of the technical report. If additional space is required, a continuation sheet shall be attached.

It is highly desirable that the abstract of classified reports be unclassified. Each paragraph of the abstract shall end with an indication of the military security classification of the information in the paragraph, represented as (TS), (S), (C), or (U)

There is no limitation on the length of the abstract. However, the suggested length is from 150 to 225 words.

**14. KEY WORDS:** Key words are technically meaningful terms or short phrases that characterize a report and may be used as index entries for cataloging the report. Key words must be selected so that no security classification is required. Identifiers, such as equipment model designation, trade name, military project code name, geographic location, may be used as key words but will be followed by an indication of technical content. The assignment of links, rules, and weights is optional